# EFFECT OF Fe₃O₄ NANOPARTICLES ON THE PREDICTION OF FERRICYANIDE CONCENTRATION BY CARBON PASTE ELECTRODE USING MACHINE LEARNING

# A THESIS SUBMITTED TO THE INSTITUTE OF GRADUATE STUDIES

## NEAR EAST UNIVERSITY

**By**

## NAJIYA MAAROF SALEEM

**In Partial Fulfilment of the Requirements for the Degree of Master of Science
in
Chemistry Department**

**NICOSIA, 2021**

# EFFECT OF $Fe_3O_4$ NANOPARTICLES ON THE PREDICTION OF FERRICYANIDE CONCENTRATION BY CARBON PASTE ELECTRODE USING MACHINE LEARNING

# A THESIS SUBMITTED TO THE  INSTITUTE

# OF GRADUATE STUDIES

# NEAR EAST UNIVERSITY

## By

## NAJIYA MAAROF SALEEM

## In Partial Fulfilment of the Requirements for
## the Degree of Master of Science
## in
## Chemistry Department

## NICOSIA, 2021

**Najiya Maarof Saleem saleem: effect of Fe$_3$O$_4$ nanoparticles on the prediction of ferricyanide concentration by carbon paste electrode using machine learning**

**Approval of the Institute of Graduate Studies**
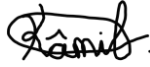
**Prof. Dr. HUSNU CAN BASER**

**We certify that this thesis is satisfactory for the award of the degree of Master of Science in Chemisrty**

**Examining Committee in Charge:**

Prof. Dr. Mehmet Özsöz          Committee Chairman, Department of Biomedical Engineering, NEU

Assoc.Prof. Dr. Kamil Dimililer       Department of Electrical and Electronics Engineering

Asst.Prof. Dr. Süleyman Aşır        Supervisor, Department of Materials Science and Nanotechnology Engineering , NEU

I hereby declare that all information in this document has been obtained and presented in accordance with academic rules and ethical conduct. I also declare that, as required by these rules and conduct, I have fully cited and referenced all material and results that are not original to this work.

**Name, Last name:** NAJIYA MAAROF SALEEM

**Signature:**

**Date:**

To my parents...

**ACKNOWLEDGEMENT**

## ABSTRACT

Electrochemical analysis methods such as electrochemical impedance, differential pulse voltammetry, and square wave voltammetry are commonly employed to characterize enzymes, proteins, and heavy metals within an extensive potential range. Carbon paste electrode (CPE) modified by iron (II, III) oxide ($Fe_3O_4$) nanoparticles were utilized for the classification of $K_3Fe(CN)_6$ using machine leaning.The voltametric data acquired from all CV, DPV, SWV measurements for different concentrations of $K_3Fe(CN)_6$ were utilized in a Gradient Boosting Algorithm (GBA) as input data. We observed from the resulting of CV, DPV, SWV measurements that the signals current of $K_3Fe(CN)_6$ increased at $Fe_3O_4$ nanoparticles modified CPE compared to unmodified CPE for LOD and $R^2$. The reason for the increase the proportion in the CV, DPV, SWVmeasurements are the high degree of conductivity of the $Fe_3O_4$ nanoparticles. The results showed that the $K_3Fe(CN)_6$ gave a linear relationship within the concentration range of 2 to 10 mM for CV ($R^2 = 0.9898$) and DPV ($R^2 = 0.9932$) and SWV ($R^2 = 0.9937$). The LOD of $K_3Fe(CN)_6$ was found 0.38 mM, 0,32 mM and 0,30 mM for CV, DPVand SWV, respectively. After analyzing the CV, DPV, SWV data by the GBA technique, Machine Learning techniques are widely used in various fields for classification purposes.A machine learning technique which is Gradient Boosting Function has been considered in order to classify the variants.  the outcomes showed that the ratio of the prediction accuracy of $K_3Fe(CN)_6$ at CPE was found as 90% , 80% and 80% for CV, DPV and SWV, respectively. In comparison, the prediction accuracy of $K_3Fe(CN)_6$ at $Fe_3O_4$ nanoparticles modified CPE was found as 97% , 75% and 82% for CV, DPV and SWV, respectively. The findings show that ML can evaluate a variety of voltammetric data, allowing for the rapid and accurate resolution of a variety of redox processes during the data processing process.

*Keywords:* machine learning; Ferric cyanide concentration; $Fe_3O_4$ nanoparticles; oxidation–reduction ; electrochemical techniques

# ÖZET

Elektrokimyasal empedans, diferansiyel puls voltametrisi ve kare dalga voltametrisi gibi elektrokimyasal analiz yöntemleri, geniş bir potansiyel aralığında enzimleri, proteinleri ve ağır metalleri karakterize etmek için yaygın olarak kullanılır. $K_3Fe(CN)_6$'nın Yapay Sinir Ağları (YSA) kullanılarak sınıflandırılması için demir (II, III) oksit ($Fe_3O_4$) nanoparçacıkları ile modifiye edilmiş karbon pasta elektrotu (CPE) kullanılmıştır. Farklı $K_3Fe(CN)_6$ konsantrasyonları için tüm CV, DPV, SWV ölçümlerinden elde edilen voltametrik veriler, giriş verileri olarak Gradient Boosting Algorithm'de (GBA) kullanıldı. CV, DPV, SWV ölçümlerinin sonucundan, $K_3Fe(CN)_6$'nın sinyal akımının, LOD ve $R^2$ için modifiye edilmemiş CPE'ye kıyasla $Fe_3O_4$ nanoparçacıkları modifiye edilmiş CPE'de arttığını gözlemledik. CV, DPV, SWV ölçümlerindeki oranın artmasının nedeni $Fe_3O_4$ nanoparçacıklarının yüksek derecede iletken olmasıdır. Sonuçlar, $K_3Fe(CN)_6$'nın CV($R^2 = 0.9898$) ve DPV ($R^2 = 0.9932$) ve SWV ($R^2 = 0.9937$) için 2 ila 10 mM konsantrasyon aralığında doğrusal bir ilişki verdiğini gösterdi. $K_3Fe(CN)_6$ için tespit limiti CV, DPV ve SWV için sırasıyla 0,38 mM, 0,32 mM ve 0,30 mM bulundu. CV, DPV, SWV verileri GBA tekniği ile analiz edildikten sonra sonuçlar, $K_3Fe(CN)_6$'nın CPE'deki tahmin doğruluğu oranının CV, DPV ve SWV için sırasıyla %90 , %80 ve %80 olarak bulunduğunu göstermiştir. Karşılaştırıldığında, $K_3Fe(CN)_6$'nın $Fe_3O_4$ nanoparçacıkları modifiye edilmiş CPE'deki tahmin doğruluğu CV, DPV ve SWV için sırasıyla %97 , %75 ve %82 olarak bulundu. Bulgular, YSA'ların çeşitli voltametrik verileri değerlendirebildiğini ve veri işleme sürecinde çeşitli redoks işlemlerinin hızlı ve doğru bir şekilde çözülmesine olanak tanıdığını göstermektedir.

*Anahtar Kelimeler:* Yapay sinir ağları; Ferrik siyanür konsantrasyonu; $Fe_3O_4$ nanoparçacıkları; yükseltgenme-indirgenme ; elektrokimyasal teknikler

**TABLE OF CONTENT**

# Contents

8

# LIST OF TABLES

# LIST OF FGURES

# LIST OF ABSERVATIONS AND SYMBOLS

| | |
|---|---|
| **µA** | Micro Ampere |
| **A** | Surface Area |
| **BMPTB** | Butyl-4-MethylPyridinium TetrafluoroBorate |
| **CE** | Counter Electrode |
| **CMCPEs** | Chemically Modified Carbon PasteElectrodes |
| **CPE** | Carbon Paste Electrode |
| **CPGrE** | Carbon Paste Groove Electrode |
| **CV** | Cyclic Voltammetry |
| **DNA** | Deoxyribo Nucliec Acid |
| **DPV** | Differential Pulse Voltammetry |
| **EMFs** | External Magnetic Fields |
| **Epa** | Anodic Peak Potential |
| **Epc** | Cathodic Peak Potential |
| **GBA** | Gradient Boosting Algorithm |
| **GCE** | Glassy Carbon Electrode |
| **Ia** | Anodic current |
| **Ic** | Cathodic current |
| **Ils** | Ionic liquids |
| **IONPs** | Iron Oxide Nanoparticles |

| | |
|---|---|
| **IOs** | Iron Oxide |
| **IVD** | In-Vitro Diagnostics |
| **LOD** | Limit of Detection |
| **LSV** | Linear Sweep Voltammetry |
| **MCPEs** | Modified Carbon Pastes Electrode |
| **mM** | Millimolar |
| **MNPs** | Magnetic Nanoparticles |
| **MRI** | Magnetic Resonance Imaging |
| **mV** | Millivolt |
| **mV/s** | millivolt per second |
| **MWCNT** | Multi-Walled Carbon Nanotube |
| **MΩ/cm** | Megaohm Per Centimeter |
| **Nm** | Nanometer |
| **PEDOT** | Poly (3,4-ethylene dioxythiophene) |
| **PGE** | Pencil Graphite Electrode |
| **RE** | Reference Electrode |
| **RTILs** | Room Ionic liquids temperature |
| **SD** | Standard Deviation |
| **SWV** | Square wave Voltammetry |
| **V** | Volt |

| WE | Working Electrode |
| --- | --- |

# CHAPTER 1
# INTRODUCTION

## 1.1. Background of Study

Electrochemical analysis Working electrode (CV), Division pulse voltammetry (DPV), and Sinewave voltammetry were utilized as techniques (SWV) to describe enzyme, protein, pharmaceutical samples, chemical compounds, and heavy metals (Guo et al., 2009). An oxidation–reduction (redox) reaction drives electrons to move from one chemical material to another in any electrochemical process. When electrons are moved from an oxidized material to a reduced material, it is called a redox reaction. The reductant is the species that loses electrons and is oxidized as a result of the reaction; the oxidant is the species that acquires electrons and is reduced as a result of the reaction. The potential difference between the valence electrons in various elements determines the corresponding potential energy. Nanomaterials are being employed to help the environment in a variety of ways. Photocatalytic copper titanium oxide nanoparticles, for example, are being studied for their breaking down oil into biodegradable chemicals. To offer a large surface area for the reaction, the nanoparticles are arranged in a grid. They can be used to clean up oil spills since they may be triggered by sunshine and operate in water. An example is gold nanostructures embedded in a porous metal oxides catalyst, which is utilized to break down volatile organic air pollutants at room temperature.. CV permits observing of oxidation/reduction reaction of chemical types, such as ferricyanide $[Fe(CN)_6]^{-3}$/ ferrocyanide $[Fe(CN)_6]^{-4}$ within an extensive potential range. The current formed at the working electrode (WE) flux via a counter electrode(CE) is observed as a triangular excitation potential is performed into the WE. The resulting voltammogram is plotted the current vs. applied WE potential comparative to the reference electrode (RE). The current signal provides information on the general rate of several processes happening at the WE surface. $[Fe(CN)_6]^{-3}$/ $[Fe(CN)_6]^{-4}$ redoxreactions couple are mainly utilized in CV, DPV, SWV measurements as a mediator carrying electrons between electroactive compounds dissolved in a solution and a WE (Cho et al., 2008). The WE are often modified by several methods: sodium dodecyl sulphate modified carbon paste electrode to detect potassium ferricyanide (Niranjana et al., 2009). PEDOT modified with copper nanoparticles to detect maleic hydrazide.

$Fe_2O_3$ nanoparticles modified CPE to detect paracetamol and dopamine (Vinay et al., 2019) ds-

DNA immobilized gold nanoparticles to detect chemicals of interest (Bard etal., 2001a) multi-walled carbon nanotube (MWCNT)/$TiO_2$ modified glassy carbon electrode (GCE) to detect potassium ferricyanide ( Perenlei et al., 2011), etc. Understanding the impacts of surface modification is significant to describe furtherthe linking of analyte molecules on the surface of the modified working electrode (Guoet al., 2009). The change of CPE with different metal oxide nanoparticles can increasethe sensitivity and selectivity and hence accelerates the electron transfer process rate between the electroactive compounds and the surface of the electrode (Vinay et al., 2019). The magnetic, optical, and electronic characteristics of $Fe_3O_4$ nanoparticles have a great significance in several industrial applications containing extended new electronic devices, information storage systems, optical devices, bioprocessing, color imaging, and the manufacture of magnetic recording media (Desmond et al., 2002).

Machine Learning are nowadays utilized in various chemistry fields, and they provide a set of techniques that might be valuable in resolving, a new area of computer science, can be applied in the electrochemical analysis, as in many science fields. The applications of ML are as significant and essential as statistical calculation or consultation depends on expert systems for the progress of electrochemical techniques. The applications' area is so extensive and differs from the Electrochemical to the advanced corrosion prediction Electrochemical applications of ML contain inhibitor design, electrochemical sensors, corrosion prediction, automatic channel inspection, electrochemical impedance spectroscopy data, electrochemical polymerization, cyclic voltammetry analysis, etc (Salari et al., 2005) In the electrochemical experimental ML are utilized to detect and monitor constituents in combinations when electrochemical results are complex through extremely overlying signals or reactions between constituents (Vlasov et al., 1997). The ML processing techniques are able to be completed by a traditional series of independent examines. On the other hand, it can be beneficial to substitute this with a statistically planned experimental procedure in which numerous features are different instantaneously. This multi-variable method decreases the quantity of tests and enhances statistical explanation of the outcomes (Zupan et al., 1993).

**1.2. Significance of the Study**

The significance of this study is apparent through using the massive number of the CV, DPV, and SWV of the ferric cyanide compound and the accelerated way of analyzing these data through using artificial intelligence, which is an element assisting the researchers in analyzing many of the chemical compounds precisely and in a very advanced and accelerated manner comparing with the human being who needs more time and efforts in collecting and analyzing these data. This study monitors the ferric cyanide compound's behavior at $Fe_3O_4NPS$ modified carbon paste electrode and bare carbon paste electrode.Nanoparticles increase the sensitivity and increase surface area and ML with cyclic voltammetry the sensitivity is increase.

Machine Learning (ML) has seen a meteoric rise in applications that solve issues and automate processes across a wide range of industries. This is mostly due to the boom in data availability, major advances in machine learning techniques, and advancements in computer power. Without a doubt, machine learning has been used to solve a variety of simple and difficult challenges in network operation and administration. There are numerous surveys on machine learning for certain networking domains or network technology. This study is unique in that it combines the use of several machine learning algorithms in several important aspects of networking across multiple network technologies. As a result, readers can gain from a detailed treatment of the various learning paradigms and machine learning approaches applied to basic networking challenges.

**1.3. Aim of the Study**

Our study aims to monitor the ferric cyanide compound's behavior at $Fe_3O_4NPS$ and modify the carbon paste electrode and bare carbon paste electrode. This study will apply the results from CV, DPV, and SWV for the ferric cyanide at $Fe_3O_4$ $NP_S$ modified Carbon Paste Electrode and unmodified carbon paste electrode in the field of artificial intelligence. Effect of $Fe_3O_4$ nanoparticles on the classification of ferricyanide concentration by carbon paste electrode using artificial neutral networks will also identified.

**1.4. Organization of study**

This research includes six parts, as shown:

Chapter 1: covers the general introduction of the topics of the study.

Chapter 2: Includes a detailed review of the main components of the study.

Chapter 3: Provides information about the contents of some of the related research and articles about the topic of study.

Chapter 4: Includes information about the materials and methods the study applied. Chapter 5: Entitles the results and provides a discussion about them.

Chapter 6: Summarizes the results obtained after conducting this study.

# CHAPTER 2

# THEORETICAL FRAMEWORK

## 2.1. Electrochemical Techniques

It is the interaction of matter with the transmission of an electric current that is based on the electron's negative characteristics. The electron, being the most important component of electricity, has a strong attraction to positively charged particles of matter, such as protons, whether they are found in atoms, groups of atoms, or molecules. This affinity is analogous to the chemical attraction that particles have for one another. Chemical reactions are caused by a shift in the electron structure of atoms, and free electrons can either join with matter particles (in a reduction process) or be released by those particles (termed as oxidation). The matters that contribute to the electrochemical reactions are named as electrolytes or ionic conductors (John et al., 1969).

## 2.2. Types of electrochemical reactions

There are several types of electrochemical reactions that can be summarized as below

## 2.2.1. Simple redox reactions

The electrical charge of a charge carrier, usually a simple or complex ion in solution, is altered in a simple redox reaction by withdrawing an electron from the electrode (reduction) or introducing an electron to the electrode (electrolysis) (termed as oxidation). It is possible for the same carriers to exist in two states of charge in solution. When the charge is higher and more positive, it is said to be oxideized, and when the charge is lower and less positive, it is said to be decreased. When there are substantial quantities of both ferric and ferrous ions in a solution, Redox equilibrium is reached at the electrode, for example, when there is a sufficiently rapid electron exchange with the electrode, giving it a well-defined potential, or reversible redox potential.

## 2.2.2. Reactions that result in gase production

In combination with additional hydrogen ions and electrons generated by metal, hydrogen is generated at the surface to make gaseous hydrogen molecules. When all reactions are sufficiently fast, a balance is attained between hydrogen ions and gas hydrogen. When such a situation happens, the hydrogen electrode reversible is a metal in contact with a solution. And their electric arc is randomly set to zero; it acts as a basis for a relative quality degradation of the hydrogen

scale, And it may be compared with all other electrodes. In the same way negative solution hydroxylate ions (OHs), which may be produced in gaseous oxygen following a number of processes, may be induced to return electrons to a metal.

### 2.2.3. Reactions that deposit and dissolve metals

The process of reducing a metal ion and of releasing it as a neutral atom or species leads to the formation of the electrode metal grid. The metals can therefore be deposited in electrodes. On the other side, when electrons are pulled out by applying positive potentials from the metal electrode, the generated metal ions can travel through the double layer of electric load, hydrate and pass on to the solution. The metal electrode will disintegrate. Many metals develop well-defined electrical potential, when in a given solution they contact their own ions.

### 2.2.4. Oxidation and reduction of organic compounds

Oxidation and reduction processes of organic compounds in electrodes can also be achieved by generating and producing products that cannot readily be transformed into the original material, which are essentially irreversible in the literal sense. However, certain molecules containing oxygen and nitrogen (quinones, amines and nitrous compounds) might avoid this rule, which has very well-defined reversible potential. *(*Aleksandaret al., 1995*)*.

### 2.3. Cyclic voltammetry (CV)

is an electrochemical method that measures the current generated under circumstances in an electrochemical cell. An electrolysis cell, a potenostat, a current to pressure converter and a data collection system are available as a system of voltammetry. The cell is comprised of an electrode, an electrode, an electrode, a cathode and an electrolytic solution that operates. The potential of the working electrode is linear to time, whereas the reference electrode has a constant potential. Electricity from the signal source to the two electrodes is conducted through the counter electrode. The objective of the electrolytic solution is the supply and reduction of ions to the electrodes. A potentiostat is an electrical device that employs a DC power supply to create a potentially retainable and precision-determinable potential and enables tiny currents to enter the system without altering the voltage. Kissinger et al. measure the resulting current with the current-to-voltage converter, and generate the results voltammogram by the data acquisition system, and can

also use a CV to determine a system electron stoichiometry and analyte diffusion coefficient, as well as an identifier for the formal reduction potential. Moreover, as the concentration in a reversible Nernstian system is proportionate to current, the concentration of an unknown solution may be measured by creating a current vs. concentration calibration curve (Kissinger P et al., 1983).
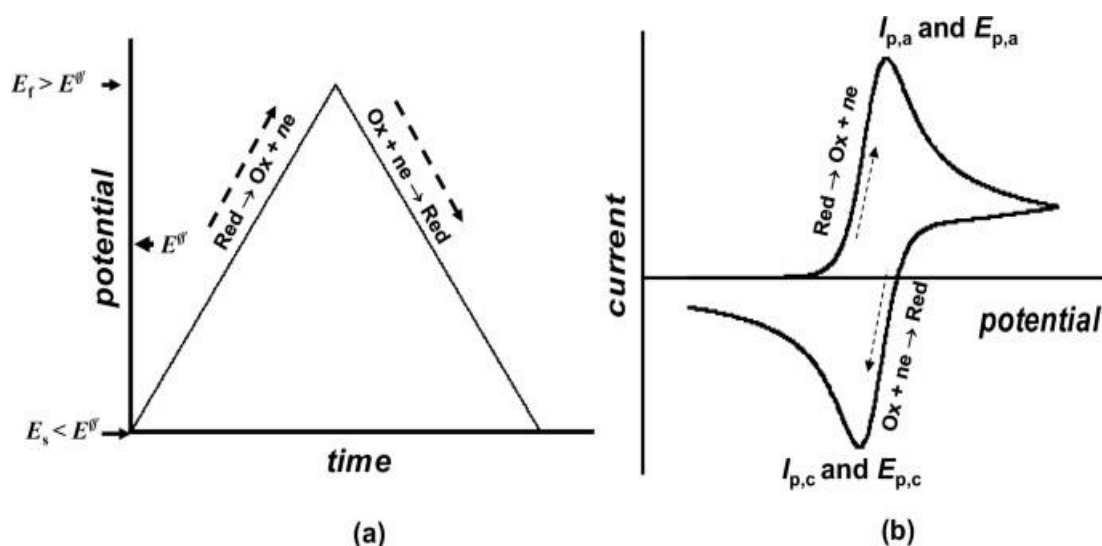


**Figure 2.1**:Potential–time excitation signal in a CV measurement and CV for a reversible oxidation-reduction process (Wang, 2006).

## 2.4. Differential pulse voltammetry (DPV)

Is an electrospinal measuring voltammetry method and a linear cyclic voltammetric sweep or staircase derivative with a number of regular voltage pulses superposed to the possible linear sweep or stair steps. It is used for cyclic voltammetry For double-potential step time chronoamperometry in a fixed planar electrode for a heterogeneous load transfer control an analytical solution is provided. Extending the result to many possible steps yields the current reaction potential for typical pulse voltammetry differentials. The reaction dependency is investigated on the exploratory parameters.

Bard et al. have shown that it is particularly important for the extended duration of the initial pulse to be dependent on the commonly used differential voltammetry methodology. According to Bard et al, when the electrogenated species are soluble in electrolytic solution, Differential pulse voltammetry at spherical electrodes of all sizes, including microelectrodes. DPV utility is therefore studied to determine the diffusion coefficients and formal potential for this aim in order to develop

optimal circumstances. Mercury microelectrodes are stated to be experimental validation of theoretical results ca. Diameters between 50 and 10 μm in both watery and ionic fluid environments. Differential Voltammetry pulse (DPV) is based on consecutive pulses of dual potential. The approach is one of the most appropriate for characterizing electrochemical systems since the nonfaradaic contribution is a picture-shaped answer (Bard et al., 2001).
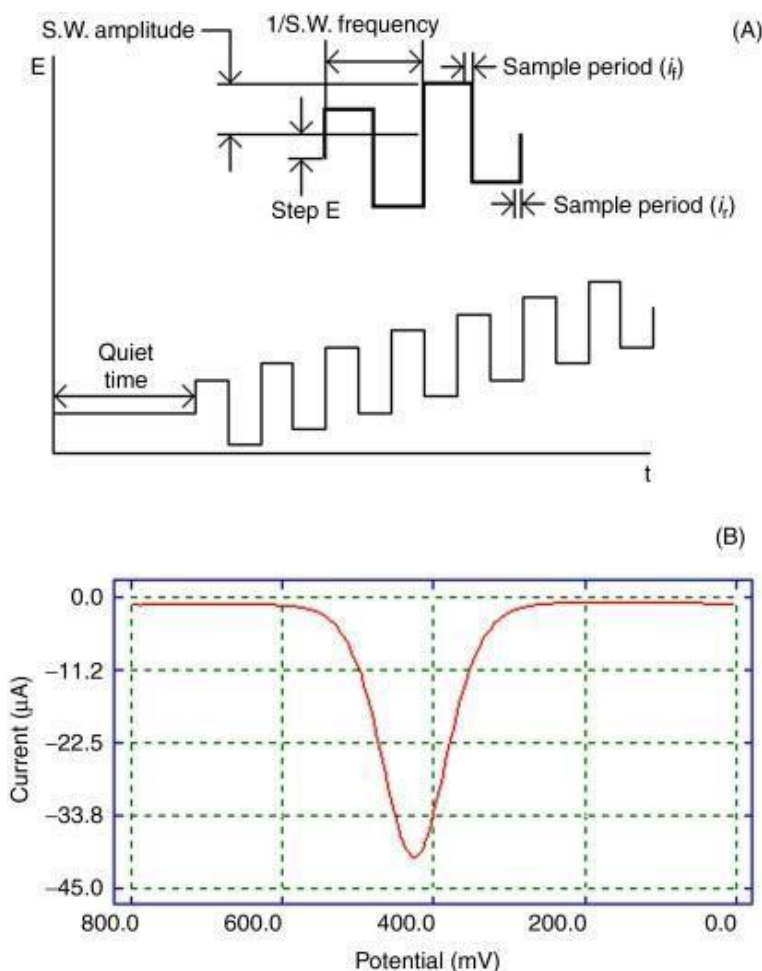


**Figure 2.2**: DPV indicating potential wave (Kissinger & Heinemann, 1996).

## 2.5. Square wave voltammetry (SWV)

Adsorbed reactants' responses are provided The SWV is shown to show its considerable sensitivity to quasi-reversible redox adsorption state processes. The links between the characteristics of the SW response and the charging transfer parameters and the stimulation signal are discussed. SWV's use has been booming in the last decade, firstly because the instruments described above are often used; secondly because of an advanced theory; and last but not least because of its great sensitivity

to the surface-confined responses of electrodes. Breiman et al. have explained that adsorbent stripping SWV is the best approach to detect electro-active chemicals adsorbed on the surface of the electrode. (Breiman et al., 1997). Electrode Process The influence of adsorbed species on the rate of an electrode reaction is proposed in a simple model. The active coefficient of the activated compound which may be determined by adsorption is supposed to express this impact. isotherm. This approach gives a reasonable account of experimental data already published and provides a framework for future experimental and theoretical work.
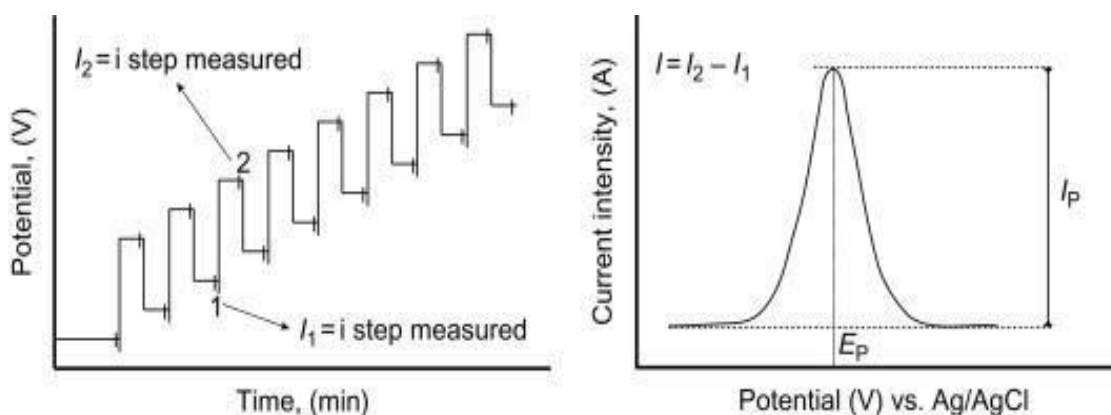


**Figure 2.3:** Potential waveform and Current sampling points at different sampling times in SWV (Kissinger & Heinemann, 1996).

## 2.6. Carbon Paste Electrode

Kuwana & French mentioned that carbon paste is composed of a suitable liquid binder, which is mixed with graphite powder Since their inception, CPEs have grown in use as a substrate in many biological and chemical modifications (Kuwana & French, 1964). CPEs exist in different forms, and most of them are made from fullerenes ($C_{60}$), pulverized diamond, glassy carbon microparticles, and acetylene blackWith such diversity, CPEs play a significant role in designing carbon nanotubes and carbon paste configurations. Todorovi et al came to the result that a binder's existence helps prevent the occurrence of different types of hydrophilic redox systems that occur during the electrode transformation process (Todorovi et al., 2009). A study by Fazi et al. State that the nature of critical components and original CPE composition affects reaction kinetics (Fazi et al., 2007). However, CPEs must possess certain binder features to serve their intended purposes

in amperometric and voltammetric applications They established that liquid pastes must have set electrochemical inactivity, long lifetime, mechanical stability as a result of low vapor pressure, and practical insolubility. Meanwhile, numerous CPEs widely used worldwide fall into a group of insulating liquids such as tri cresyl phosphate, bromonaphthalene, silicon oil, and paraffin oil. According to Klinkenberg et al and Schultz and Kuwana, ionic liquids (ILs) can also serve a critical binder purpose when used to prepare CPEs (Klinkenberg et al., 2003; Schultz & Kuwana, 1965). But the significant difference is that these ILs can either function at room temperature or gazetted temperatures and thus giving rise to ILs and room ionic liquids (RTILs). Todorovi et al mentioned that considerable attention has been placed towards the study of RTILs because they have excellent biocompatibility, enhance direct electron-transfer, and huge electrochemical potential window (Todorovi et al., 2009). According to both Morais et al and Shi et al, they are also desirable because of their soluble in organic and inorganic molecules, have high conductivity, chemical stability, high thermal power, negligible vapor pressure, and other distinct physical features (Morais et al., 1981; Shi et al., 2008). An earlier study by Schultz and Kuwana considered them to be necessary because of their ability to serve as either a solvent or an electrolyte (Schultz and Kuwana, 1965). Hence, Klinkenberg et al contend that these features are vital in both analytical electrochemistry and electrochemistry (Klinkenberg et al, 2003).

Nevertheless, and in referrence to results of a study by Shi et al, IL-based pastes do not always have a high analytical utility, and this is because of their high background current (Shi et al., 2008). Klinkenberg et al and Morais et al highlighted that there have been considerable efforts meant to examine ways that can be used to determine the best CPE elements as well as testing the effectiveness of newly formed electrodes (Klinkenberg et al., 2003; Morais et al., 1981). Inferences from these studies revealed that electrodes can be modified wholly or on the surface and that either type of modification used has distinct effects on the electrode's performance. This implies that different results are most likely to be obtained when studies involving the use of differently modified CPEs are conducted. However, and as Todorovi et al has explained the notable inference that can be made is that changing the electrode to suit the desired properties is advantageous and associated with specific inherent challenges (Todorovi et al., 2009). A study by Fazio et al established the same idea and noted that differently modified CPEs tend to exhibit different behavior forms in the same situation (Fazio et al., 2007). Hence, changing CPEs to detect ferricyanide is mostly going to provide various deductions and research implications.

Klinkenberg et al highlighted that CPEs have better characteristics and offer many advantages compared to other traditional electrodes. As a result, studies often consider and prefer to use CPEs when conducting voltammetric measurements also, established that new sensors of the desired features are easily obtainable on a quantitative scale following the use of modified CPEs. In addition, consider that numerous and specific milestones and achievements can be made using modified CPEs to conduct voltammetric measurements (Klinkenberg et al., 2003). Fazio et al asserted that CPEs exist either as chemically modified or unmodified CPEs and that each group has its specific implications on obtainable voltammetric measurements. The same resource also showed that three critical variants used to modify CPEs biologically and these are (Fazio et al., 2007).

Sugiyama et al and Varma el al accepts no argument that CPEs are cost-effective compared to other forms of electrodes, and also point out the aspect of CPEs being in a position to allow the production of electrodes of the desired features (Sugiyama et al., 2000; Varma et al., 2004). Morais et al repots that the desired CPE features are a product of a combination of the best electrochemical and physicochemical characteristics (Morais et al., 1981). Which is, according to Sugiyama et al, it is one of the main reasons as to why CPEs are widely utilized as highly selective sensors in organic and inorganic electrochemistry (Sugiyama et al., 2000). The other thing to note with CPEs is, according to Todorovi et al, is that they exhibit some form of heterogeneous behavior, which is influenced by a liquid binder (Todorovi et al., 2009). Hence, all the existing and various CPEs of different features require reliable and vast characterization methods. Todorovi et al provides a pictorial description of the CP groove electrode (CPGrE) as normal construction of CPE, which replicates screen-printed electrodes' planar structure (Shi et al., 2008).



**Figure 2.4:** Carbon Paste Electrode CPE

A CPGrE is made up of plastic inserts, a metal contact, and a small plastic prismatic bar, which is used to fill the carbon paste. Todorovic et al that the required surface area can be obtained using ordinary plastic pipette tips and giving rise to what is termed CPmE (Carbon Paste Mini-Electrode) (Todorovic et al., 2009). This type of electrode serves an essential function as it does not quickly get its surface area consumed, making it economical compared to carbon nanotubes, which are expensive.

## 2.7. Potassium Ferric Cyanide

Potassium ferricyanide is a chemical compound with the formula of $K_3[Fe (CN)_6]$. Gmelin and Leopold describes it as a salt with a bright red color, soluble in water, and its solution shows a green- yellow fluorescence (Gmelin and Leopold, 1822). The compound that was discovered by Leopold Gmelin in 1822 was used at the beginning of producing ultramarine dyes. Potassium ferricyanide is used in the physiology field as a way of increasing the redox potential of a solution. So, it can oxidize the reduced cytochrome c in intact separated mitochondria. Carson mentiones that Potassium ferricyanide is also used to determine the ferric reducing power potential of an extract of a chemical compound and other samples (Carson, 1997). CV, DPV, SWV of potassium ferricyanide are model electrochemical system to study a reversible redox system's behavioral patterns without facing the difficulty of different analytical techniques.

## 2.8. Structure of the Potassium ferric cyanide

Gmelin and Leopold state that the solid potassium ferricyanide has a complicated polymeric structure which is composed of octahedral $[Fe(CN)_6]^{-3}$ centers linked with potassium ions that are bound to the CN ligands (Gmelin and Leopold, 1822).

## 2.9. The basic idea behind nanoparticles

Laws and principles of quantum mechanics influence the existence, use, and functions of nanoparticles. Hence, a nanoparticle can be defined based on a quantum mechanics perspective as an ultrafine particle whose sizes range from 1 to 100 nm. Concerning industrial applications, it is apparent that the diverse features of nanoparticles are desirable for use in many applications. NPs have specific magnetizations, mechanical strengths, optical properties, high surface area, and low melting point features, making them highly applicable in a number of industrial applications. However, it must be noted that the characterization of NPs is determined by the specification under

which they fall, and which according to Drexler, can be depicted using a distinction between nanomaterials and nanoparticles as well as specifications (Drexler, 1986).

## 2.10. Iron oxide nanoparticles

Iron oxide nanoparticles (IOs) exist in different forms, and there are about 16 types of IOs, including oxide- hydroxides, hydroxides, and oxides. They all resemble one common feature in the sense that they are all-natural compounds, but they can be synthesized using stipulated experimental procedures. Wu, He, and Jiang outlined that the entire crystal structure and valency play a vital role in distinguishing oxides though they can have similar hydroxide (OH), oxygen (O), and iron (Fe) composition (Wu, He, and Jiang ., 2008). Some of the notable IOs widely used in many industrial and experimental processes include hematite, magnetite, lepidocrocite, akageneite, and goethite. Teha and Koh established that IONPs have diameters ranging from 1 to 100nm and can be used in several activities such as drug-delivery, biosensing, and magnetic data storage (Teha and Koh, 2009). Nevertheless, and as Roh et al describes, IONPs are made up of magnetite ($Fe_3O_4$) and maghemite ($\gamma$- $Fe_2O_3$), and their surface area tends to increase in response to changes in volume (Roh et al., 2006). As a result, IONPs have high dispersibility and binding potential. On the other hand, the lack of external magnetic fields (EMFs) reduces the magnetization of magnetic NPs (MNPs) to 0. This applies significantly to NPs whose display super-Para magnetism falls within 2 and 20 nm. Thus, and according to Bharde et al, efforts to ensure that MNPs remain stable when disposed of in a solution require that they are magnetized using external magnetic sources, and this is advisable when there is no EMFs present (Bharde et al., 2008).

In a study by Apetrei & Apetrei (2016), it was noted that IONPs are non-toxic and have high biocompatibility (superparamagnetic properties), which make them suitable for use in several biomedical processes. In the same study, it was also noted that there had been some considerable advancements in the use of thermal decomposition to prepare IONPs. Such developments have resulted in better IONPs in terms of their crystalline structure, monodispersity, size, and tunability. Furthermore, Apetrei and Apetrei (2016) assert that bio-accessible and water-soluble IONPs can be developed using organic ligand-coated, hydrophobic, and monolayer polymer coating methods. Gupta and Gupta find this important because they can be used in conjunction with different biomolecules at high temperatures and pH levels while maintaining a high stability level (Gupta & Gupta, 2005).

On the other hand, other methods comprising various biocompatible coatings such as lipid molecules and polysaccharides are also being developed, which, according to Wu et al, has proved to be important in drug and food administration (Wu et al., 2008). Moreover, Apetrei and Apetrei informs that new and improved ways of developing NPs related applications are being facilitated by an increase in research aimed at improving the standards of water-soluble and organic IONPs. Important examples can be drawn by Apetrei & Apetrei (2016) from the following activities and processes (Apetrei & Apetrei, 2016);

1.In antibody and vaccine production when used as nano adjuvants.

2.In-vitro diagnostics (IVD) by using them as magnetic sensing probes.

3.Hyperthermia-based cancer treatments by using them as therapeutic agents.

4.In gene therapy, when used as gene carriers.

5.For specific drug delivery since they can be used as drug carriers.

6.Magnetic Resonance Imaging (MRI) when used as contrast agents.

According to Bharde et al, there has been some notable growth in the number of studies aimed at improving the monodisperse, biocompatible, size and shape-controlled IONPs used in magnetic theranostic applications. This studies focused on using methods such as microorganisms and bacterial, electrospray, electrochemical, synthesis, microemulsion, sonochemical, sol-gel, thermal decomposition, hydrothermal, and co-precipitation synthesis. But the size and morphology of the IONPs are influenced by the pressure and temperature applied during the synthesis process (Bharde et al., 2008). Laurent et al mentioned high pressure and temperatures exceeding 2000 psi and 200 °C can be used in autoclaves or reactors for hydrothermal synthesis purposes in aqueous media (Laurent et al., 2008). Willard et al mentioned that the structure and shape of the IONPs can be controlled by thermally decomposing hydrothermal and precursors at a temperature exceeding 300 °C. Such temperatures are essential for enhancing and managing the solubility, growth, and nucleation of the NPs (Willard et al., 2004). This is mostly done when one wants to produce NPs which are narrowly and uniformly distributed.
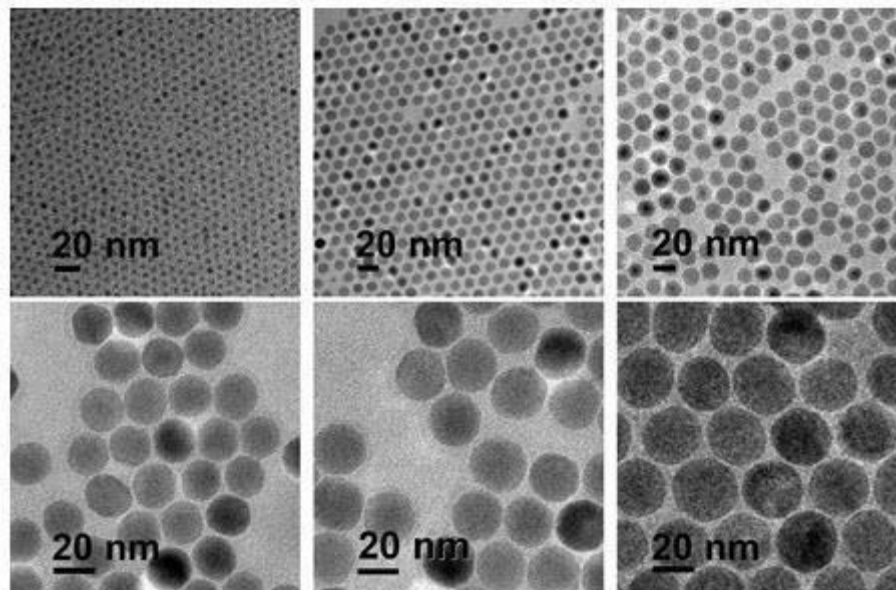
**Figure 2.5:** Shape, Size and Structure-Controlled Synthesis of IONanoparticles (Xie et al., 2018)

Willard et al have agreed that the use of various synthesis methods has resulted in numerous IONPs with different morphology and monodisperse such as multi branches, octopods, concaves, octahedrons, truncated octahedrons, cubes, tetrahedrons, plates, and nanospheres. The thermal decomposition process will result in co-authors and Hyeon synthesized iron oxide nanocrystals of various weights in each reaction. Self-assembled, multibranched, concave, octahedrons, tetrahedrons, and plate structures (A, B, C, E, G, and I) were produced using reaction temperature the use iron oleate/sodium oleate as depicted in Figure 2.5 (Willard et al., 2004). Kovalenko et al went the same direction and agreed that the process involved using sodium oleate to carry out a series of thermal decomposition of iron oleate. This led to the development of other ways of conducting metal oxide NPs controlled synthetization (Kovalenko et al., 2007). In another study, Zhao et al used 1-octadecene solvent to decompose iron oleate to synthesized Octopod IONPs (Zhao et al., 2013). This led to the production of shape and size-controlled cubic iron oxide nanocrystals. He et al used polyethylene glycol 400 and a surfactant-assisted hydrothermal route in a study aimed at examining the synthetization of 1-dimensional and 3-dimensional structures IONPs (He et al., 2007). The process's end product was single-crystal $Fe_3O_4$ (nanowires), which were ultra-thin and uniform and a diameter that averaged 15 nm (see Figure 2.5). The study was based on a previous study performed by Liu et al which controlled the wall thickness, diameter, and length of the NPs (Liu et al., 2005).
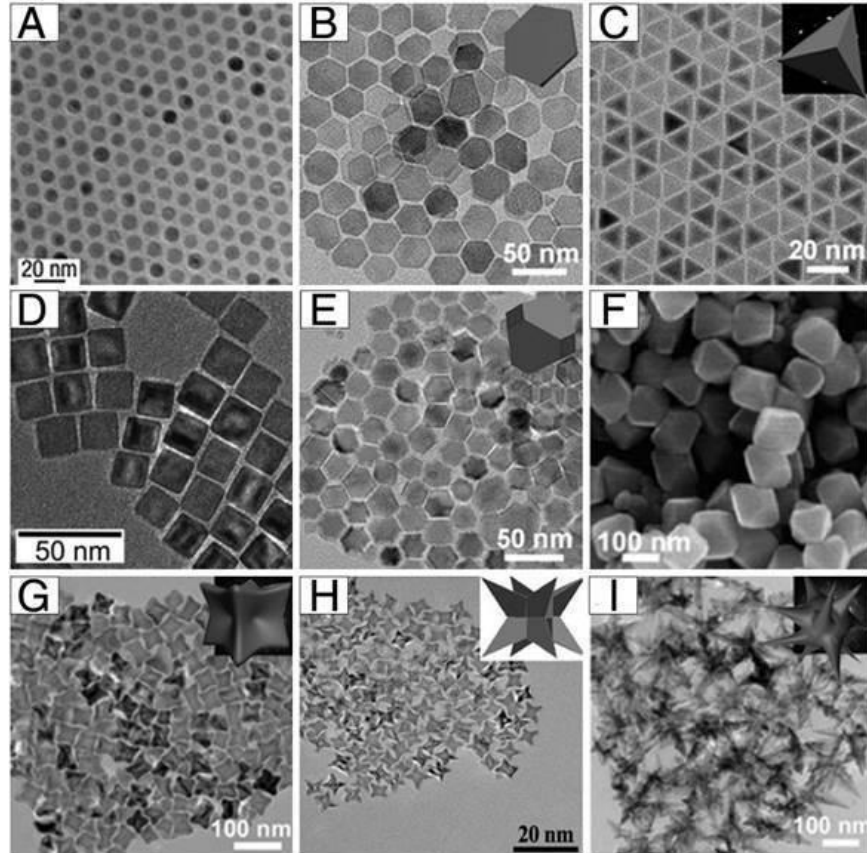
**Figure 2.6:** Morphological examples of 0-dimensional IONPs(A) nanospheres, (B) plates, (C) tetrahedrons, (D) cubes, (E) truncated octahedrons, octahedrons, (G) concaves, (H) Octapods, and (I) multi branches (Xie et al., 2018).

Zhen et al used microwave-assisted and wet-chemical etching approaches to produce magnetic IONPs . The procedures involved the use of controlled $Fe_3O_4$ nanotubes and MgO cores. The latter had its diameter and length tuned to facilitate thedeposition process. The precursor particles were formed as a result of the continued supply of energy provided by the microwave-assisted method. It was noted that the formed NPs had a high aspect ratio figure 2.6 (Zhen et al, 2007).

Wan et al conducted an experiment that encompassed setting temperatures to 120 °C for 20h so as to facilitate the use of a soft-template-assisted hydrothermal route.The investigation resulted in the preparation of $Fe_3O_4$ nanorods whose length and diameter averaged 200 nm and 25 nm, respectively. The formation of the single-crystal$Fe_3O_4$ nanorods was facilitated by using benzene, which helped to prevent oxidation. In addition, the process also required the use of a soft template that was provided by ethylenediamine (Wan et al., 2005). Jia et al used temperatures ranging from 220°C for 48h to conduct a relatively similar experiment. 0.02M of $FeCl_3$ solution was

hydrothermally treated, and the process resulted in the formation of single-crystal hematite nanotubes (Jia et al., 2013).A subsequent study by Jia et al produced in the production of single-wall $Fe_3O_4$ NPs with a length, inner diameter, and outer diameter of 250-400 nm, 40-80 nm, and 90-110 nm, respectively; the formation of the single-crystals and other structures encompassed subjecting the ellipsoid precursors to multisite dissolution. It was further noted that cheaper and high-quality elliptical $Fe_3O_4$ nanorings are obtainable using microwave-assisted hydrothermal procedures. The nanorings had better interference, micro antenna radiation, oscillation resonance absorption, multi resonance, dielectric loss, and microwave absorption properties (Jia et al., 2007).
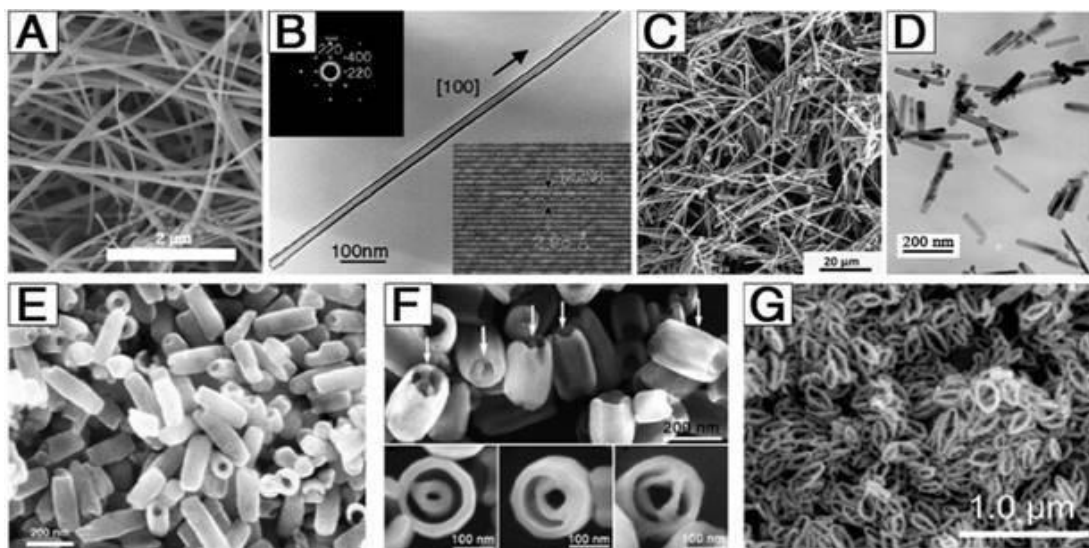


**Figure 2.7:** Morphological examples of 1-dimensional and 3-dimensional IONPs(A), nanowires, (B) long nanotubes, (C) nanoneedles, (D) nanorods, (E) short nanotubes, (F) tube-in-tubes, and (G) nanorings (Xie et al., 2018)

## 2.11. Conductivity of IONPs

Conductive electrodies and electrical circuits that stay stable under recurrent mechanical pressures are extremely desirable and generally applied in the new era of flexible display technology. The design of these materials is mutually exclusive in terms of flexibility, electrical conductivity and strength. Insulation techniques are generally utilized when the conductive material, for example in the case of electric cables, is coated with a flexible elastomer. New ways to include the leading material in the reinforcement structure are being developed which enable an electric current to be operated by the normally non-conductive material. To that end, the utilization of SBS rubber fiber material coated with silver nanoparticles was studied under an article by PARK et al. With the

resultant material, efficient conductivity was maintained while significant deformations were overcome. Antennas or wearable electronics are available for these applications. (Park, 2012).

## 2.12. Artificial Intelligence

It is the intelligence of machines, on the contrary of human natural intelligence. The field of artificial intelligence investigates intelligent agents that include devices that sense the environment and take activities to maximize their chances of effectively achieving their objectives. Poole et al. argues that artificial intelligence is generally used to characterize machinery having the same "cognitive" activities, such as "learning" and "problem solving," that human beings identify with the human mind. (Poole et al., 1998). If the capacity of these computers improves, any "intelligent" task is normally eliminated from the definition of Artificial Intelligence, a unique phenomena known as the "AI" effect. The ability of current computers usually considered to be Artificial Intelligence include the know-how of the human voice, competing on the highest level in strategic gaming systems, running automobiles autonomously and simulating military action. The fresh and updated approaches of artificial intelligence are all too many. Smith presented numerous examples of Artificial Intelligence as follows, not just (Smith, 2016).

-Autonomous cars

-Health and medical diagnoses

-Art Creation

-Mathematical theories

-Game playing

-Online searching engines

-Online support

-Recognizing images in photographs

-Filtering spams

-Online advertisements

The artificial intelligence area was essentially founded in 1955 as a university discipline. Most of its history has been split into sub-fields that generally fail to communicate with one another. They are centered on technological aspects, such as particular objectives, such as the learning of robotics. Any simple neuron receives a weight of vote against it or if this neuron activates itself when it is triggered. The new neural networks can learn both the digital and continuing functionalities.Russel et al described that the neural networks' early successes included imagining the stock market and a mostly self-driving vehicle (Russel et al., 2003). Asir et al, in one of the studies has described that sometimes, The cyclic voltammetry (CV) together with ML are integrated and explored as an analytical technique for simultaneous quantification using pencil graphite electrode of potassium ferricianide (PGE). Two parts explained the technique involving CV and ANN. In the first case, CVs with sufficient analysis information provide complex signals comprising information on the chemical with varying peak intensities for different sample concentrations. In the second part of the training an ANN was developed for the accurate interpretation and simultaneous analysis of the multi-variable signals given in voltammogrammes. considered interferences (Asir et al., 2019).

## 2.13 Gradient boosting Algorithm (GBA)

Gradient boosting is a machine learning technique for regression and classification problems, which produces a prediction model in the form of an ensemble of weak prediction models, typically decision trees. It builds the model in a stage-wise fashion like other boosting methods do, and it generalizes them by allowing optimization of an arbitrary differentiable loss function. The idea of gradient boosting originated in certain observations that boosting can be interpreted as an optimization algorithm on a suitable cost function. Explicit regression gradient boosting algorithms were subsequently developed, simultaneously with the more general functional gradient boosting. These two observations introduced the view of boosting algorithms as iterative functional gradient descent algorithms. That is, algorithms that optimize a cost function over function space by iteratively choosing a function (weak hypothesis) that points in the negative gradient direction. İn a study by Friedman et al, there was a conclusion that this functional gradient view of boosting has led to the development of boosting algorithms in many areas of machine learning and statistics beyond regression and classification (Friedman et al., 1999).

## 2.14. Modified carbon pastes in stripping analysis

CPs are the most important and appropriate material for the preparation of modified electrodes. In conducting stripping analyses, changed as well as unmodified CPs are also essential. In order to examine the function and consequences of CPE in the determination of chemical substances, it is therefore always vital to investigate both situations. In a research comprising a binding and dissolved modifier, the homogenization procedure requires a CP. For example, this work has discovered that cobalt (II) phthalocyanine and modified carbon electrode paste may be determined to use ascorbic acid present in food. (mCPE) (Kalcher et al., 1999). In addition, the modifying procedure ensures the optimal use of the electrode paste surface. In another Galík et al. research, it was observed that in such a setting the creation of negatively charged complex anions is conceivable (Galík et al., 2007). Galik et al. further stress that chromium (VI) (Galík et al. 2006) is important in defining the significance of mCPEs. These thoughts emphasize the importance of mCPEs for stripping and therefore highlight the value of this work in investigating the importance and role of mCPEs in determining ferricyanide.

# CHAPTER 3
# RELATED RESEARCH

## 3.1. Releated Researches

Jelechem et al. (2019) carbon paste electrode (CPE) modified by sodium dodecyl sulphate (SDS) was used for the detection of $K_3Fe(CN)_6$ and dopamine. Cyclic voltammetry (CV) demonstrated improved response of $K_3Fe(CN)_6$ and dopamine sensor at SDS/CPE compared to bare CPE. The effect of SDS concentration on the electrode quality also reveals that SDS formed a monolayer on a carbon paste electrode surface with a high density of negative charged end directed outside the electrode. On the formation of a SDS monolayer, the structure of the electrode interface changed significantly and the electrode/solution interface was replaced by the SDS monolayer/solution interface. The detection limit for $K_3Fe(CN)_6$ is $1\times10^{-4}$M and dopamine $1\times10^{-7}$M.

Wiley et al. (2004) The 1-butyl 4-methyl pyridinium tetrafluoro borate (BMPTB) modified carbon paste electrode (CPE) was utilized to detect $K_3Fe(CN)_6$ and dopamine. In comparison to the naked CPE with different forms of cyclic voltams, the cyclic voltamm method exhibited a very better response of $K_3Fe(CN)_6$ and dopamine in the BMPTB/CPE. The influence of BMPTB's focus on the quality of the electrode also indicates that BMPTB developed on a highly densely packed CPE surface outside the electrode. A limit of 1 1 bis$10^{-4}$ M and dopamine 1 bis$10^{-5}$ M is set for the modified electrode of $K_3Fe(CN)_6$.Lu et al. (2006) used hemoglobin and horseradish peroxides as part of direct electrocatalysis and electrochemistry investigation of Chitosan composite film/RTIL.

Zhao et al. (2013) had previously conducted a relatively similar study involving a modified carbon nanomaterials composite film electrode.

Yang et al. (2006) used related materials in solutions involving ascorbic acid, uric acid, and a binder in the form of RTIL to determine dopamine. Both studies showed that CPEs tend to exhibit good chemical behavior. The study also revealed that RTIL is vital for electrocatalysis and electrochemistry because of its high ionic conductivity and viscosity.

Maliki et al. (2006) conducted a study aimed at enhancing electron transfer using an mCPE that was made up of octylpytridinium hexafluorophosphate. The research established that mCPEs assist

in improving electron transfer when used together with appropriate solutions such as octylpyridinium hexafluorophosphate. The results also implied that using a wrong or inappropriate answer or substances can cause a reduction in electron transfer.

Sun et al. (2007) attempt to use ionic liquid CPE that contains sodium alginate hydra-gel, which acts as a form of an immobilizer to examine the electrochemistry of hemoglobin The study involved the use of 1-butyl-3-methylimidazoliumhexafluro phosphate mCPE. It was noted that mCPEs provide a powerful examination method of hemoglobin with a detection rate exceeding 89%.

Wei Sun et al. (2007) also conducted a relatively similar study to the one by Sun et al. (2007). However, Wei Sun and others' studies extended focus towards examining the analytical application and electrocatalytic activity of liquid mCPEs. The materials used included dopamine and ionic liquid 1-butyl-4-methyl pyridinium tetrafluoroborate. The findings showed that dopamine could also be used as a suitable sensor and neurotransmitter, especially in potassium ferricyanide solutions.

Pandurangachar et al. (2010) conducted a cyclic voltammetric analysis of an mCPE and 1-butyl-4-methyl pyridinium tetrafluoroborate (BMPTB) to examine dopamine and $K_3Fe(CN)_6$. It was established that dopamine and $K_3Fe(CN)_6$ showed high responsiveness when used together with CPEs combined with (BMPTB). Ordinary CPEs were noted to have low reactivity when used alone to conduct the voltammetric tests. Besides, the results also confirmed that a negative charge of high density was formed on the CPE surface as a result of the presence of BMPTB. Meanwhile, various shapes of cyclic voltammograms were produced for tests conducted using an ordinary CPE.

Shabani, Lakhaiy Rizi, and Moosavi (2018) utilized a mCPEs that was modified with IONPs to determine isoniazid ultra-trace using potentiometric sensors. The idea was that different electrodes had got different selectivity, sensitivity, and precision. As such, the results reaffirmed that $Fe_3O_4$/mCPEs had reached a high capacity to provide better voltammetric selectivity, sensitivity, and accuracy. The study also focused on determining the best possible pH conditions that offer the highest electrode response level and for interfering ions. The results reaffirmed that the best possible pH condition provides the highest level of electrode response and interfering ions. As

such, that pH was identified to be 6.5, and the desired electrode was composed of 0.012g magnetic NPs, 0.006g silicon oil, and 0.060g graphite powder.

Çubuku Timur and Anik (2007) conducted a detection of hypoxanthine and xanthine using a glassy CPE modified with xanthine oxidase and gold NPs. Hypoxanthine and xanthine were characterized before they were used to optimize the system as part of the biosensors' preparation. Hypoxanthine and xanthine were discovered to have linear trends for concentrations of $5.00 \times 10^{-7}$ and $1.00 \times 10^{-5}$, respectively. Both engagements were put in solutions containing CPEs modified with gold NPs and another with an unmodified CPE. The test results showed higher detection capacity in a concentration containing CPEs modified with gold NPs compared to a concentration containing an unmodified CPE. The same approach also showed similar results when it was used to detect xanthine in canned tuna fish.

Shahrokhian and Asadian (2010) used mCPEs, and thionine immobilized multi-walled carbon nanotube to conduct a simultaneous determination isoniazid, acetaminophen, and ascorbic acid. The procedures involved the use of voltammetric and differential pulse analysis. Both acetaminophen and ascorbic acid were observed to play an essential catalytic role in both the voltammetric and differential pulse analysis. In addition, both compounds were noted to be having a peak resolution of ~303 mV. However, isoniazid was discovered not to be having a significant effect on drug interference. The mCPEs were also observed to be having different pHs and sweep rates.

In light of all these empirical findings, it can thus be inferred that the determination of $K_3[Fe(CN)_6]$ will vary between the type of electrode used to conduct both the potentiometry and voltammetry analysis. In particular, mCPEs and ordinary CPEs have different implications on the determination of a chemical compound. However, mCPE has got a higher selectivity, sensitivity, and precision as compared to unmodified CPEs. Expectations are that the best possible pH conditions that offer the highest level of electrode response and for interfering ions will range from 6.0 to 6.5. Besides, the study further expects the desired electrode to be composed of 0.012g magnetic NPs, 0.006g silicon oil, and 0.060g graphite powder. This is in line with deductions that can be made from the reviewed related studie

# CHAPTER 4

# MATERIALS AND METHODS

## 4.1. Materials

### 4.1.1. Materials

Voltametric measurements were carried out using AUTO LAB PGSTAT 204 (Utrecht, The Netherlands) potentiostat with NOVA 2.1.2 software (Figure 4.1). Magnetite iron oxide ($Fe_3O_4$) nanoparticles modified carbon paste electrode (CPE) was used as a active electrodes (WE), a pipette tip was employed as a counter electrode (CE), and the Reference electrode (RE) was an Ag/AgCl. All the electrochemical experiments were done under room temperature at 25˚C.
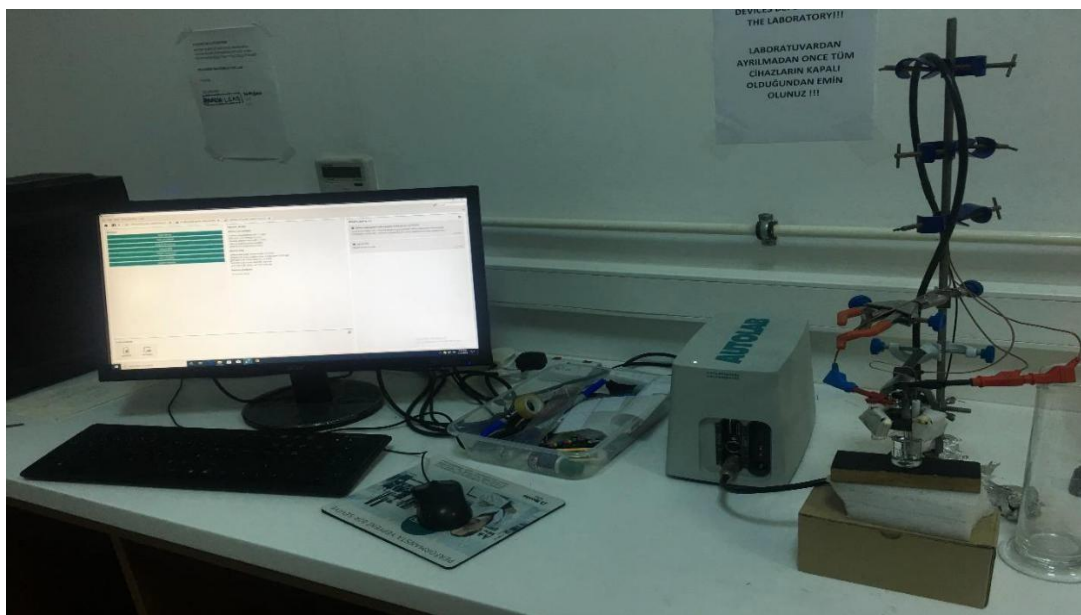


**Figure 4.1:** AUTO LAB PGSTAT 204 potentiostat with Nova 2.12

### 4.1.2. Chemicals

Powding ferricyanide was produced from Sigma, $K_3Fe(CN)_6$ and potassium nitrate, $KNO_3$. A deionized water (18.2 M a/cm) was used to produce acetate buffer solution (pH 7) and also a 500 mL stock solution of 10 mM $K_3Fe(CN)_6$ was created in 0.1 M $KNO_3$. $Fe_3O_4$ has been utilized for the production of nanoparticles, paraffin oil and carbon powder. The $K_3Fe(CN)_6$ (2, 4, 6, 8, 10 mM) was produced at different levels at 0.1 M $KNO_3$. The analytical grade was all the substances utilized.

### 4.1.3. Preparation of Working Electrode

The carbon paste electrode (CPE) was formulated by blending 0.06 g of the graphite powder with 0.04 g of the paraffin oil utilizing a mortar and pestle. Magnetite ($Fe_3O_4$)nanoparticles modified CPE was formulated by blending 0.076 g of the graphite powder, 0.02 g paraffin oil, and 0.004 g $Fe_3O_4$ nanoparticles, and the resultant blend was completely homogenized utilizing a mortar and pestle. The resulting paste was accordingly filled inside a Teflon tip (outer diameter 3 mm) and a platinum wire put inside the paste. The open end of the surface electrode was cleaned utilizing paper to obtain a reproducible smooth working surface electrode.

### 4.2. Methods

### 4.2.1. General Procedure for Voltammetric Measurements

The electrochemical determination of Potassium ferricyanide was elucidated using theCV, DPV, and SWV methods in the acetate buffer system. Each voltammetric methodexperiment was applied twenty times for each concentration from all $K_3Fe(CN)_6$ , the electrode reactivated through a sheet so that the electrode was smooth after each experiment. 10 mL of different levels (2, 4, 6, 8, 10 mM) of $K_3Fe(CN)_6$ were used and transferred into the electrochemical cell. All method examinations were carried out with this method by the following parameters for CV: The potential start is -0.4 V; the potential stop is -0.4 virgin; the top vertex potentials are 1.2 V; the bottom possible vertex -1.2 V and the scan rate is 100 mV/s. Amplitude of modulation 0.025V, duration of modulation 0.05s, time of the 0.5s and time of the SWV interval potential 0V, stop potential 1V, stage 0.004 V, amplitude of modulation 0.02 V and frequency 2 Hz.

### 4.2.2. Gradient Boosting Algorithm GBA Procedure

The voltammetric data acquired from all CV, DPV, and SWV measurements were utilized in a Gradient Boosting Algorithm (GBA) as input data. The GBA was performed using a combined set of 100 experiments comprising different concentrations, which were repeatedly carried out twenty times using $Fe_3O_4$ nanoparticles modified CPE. Also, 100 investigations involving different levels were regularly carried out twenty times using unmodified CPE. After each voltammetric method measurement, data were acquired and utilized in the machine learning (ML) technique. Data for the cyclic voltammetry was obtained from the anodic and cathodic signals of $K_3Fe(CN)_6$ .Cyclic voltametry Formulated data were anodic peak potential, cathodic peak potential, peak height, peak

width, peak area, peak (1/2), base start, base end, and peaksum of derivatives for each anodic and cathodic signal, Data on DPV,SWV, peak height, peak region, base start, baseline beginning, peak width(1/2), peak (1/2) peak total, were derived from peak positions.

# CHAPTER 5
# RESULT AND DISCUSSION

## 5.1. Electrochemical Behavior of Potassium Ferricyanide at $Fe_3O_4$ nanoparticles modified CPE

The potassium ferricyanide redox probe's redox reaction was used to monitor the electrochemical behavior of $Fe_3O_4$ nanoparticles modified CPE and unmodified CPE.Figure 5.1 demonstrates the CV measurement has obtained: (a) CPE; (b) CPE 2 mM of $K_3Fe(CN)_6$ with $Fe_3O_4$ nanoparticles composed of 0.1 M $KNO_3$ solution. A peak-to-peak potential separation (THEP) of 160 mV for $Fe_3O_4$ modified CPE nanoparticles and 260 mV for non-cPE is present in the obtained CV of $Fe(CN)_6^{3-}$ / $Fe(CN)_6^{4-}$ pair.The observed estimation of $\Delta Ep$ has been increased at unmodified CPE when it appeared differently concerning $Fe_3O_4$ nanoparticles adjusted CPE. It is shown to the reversible process at $Fe_3O_4$ nanoparticles modified CPE than unmodified CPE. Besides, we observed from the figure that the reduction and oxidation for $Fe(CN)_6^{3-}$/ $Fe(CN)_6^{4-}$ the couple have been better at $Fe_3O_4$ nanoparticles modified CPE than the oxidation/reduction reaction unmodified CPE. The expansion in $\Delta Ep$ amount with a reduction in signal current indicated the total CPE had diminished surface area than $Fe_3O_4$ nanoparticles modified CPE; this might be the existence of $Fe_3O_4$ nanoparticles,upgrades the pace of electron relocation. We observed that the increase in the signal in the cyclic voltammetry measurement is the high degree of electrical conductivity ofthe $Fe_3O_4$ nanoparticles; this is due to the presence of two oxidation states lead to an increase in the electron transfer process.

.
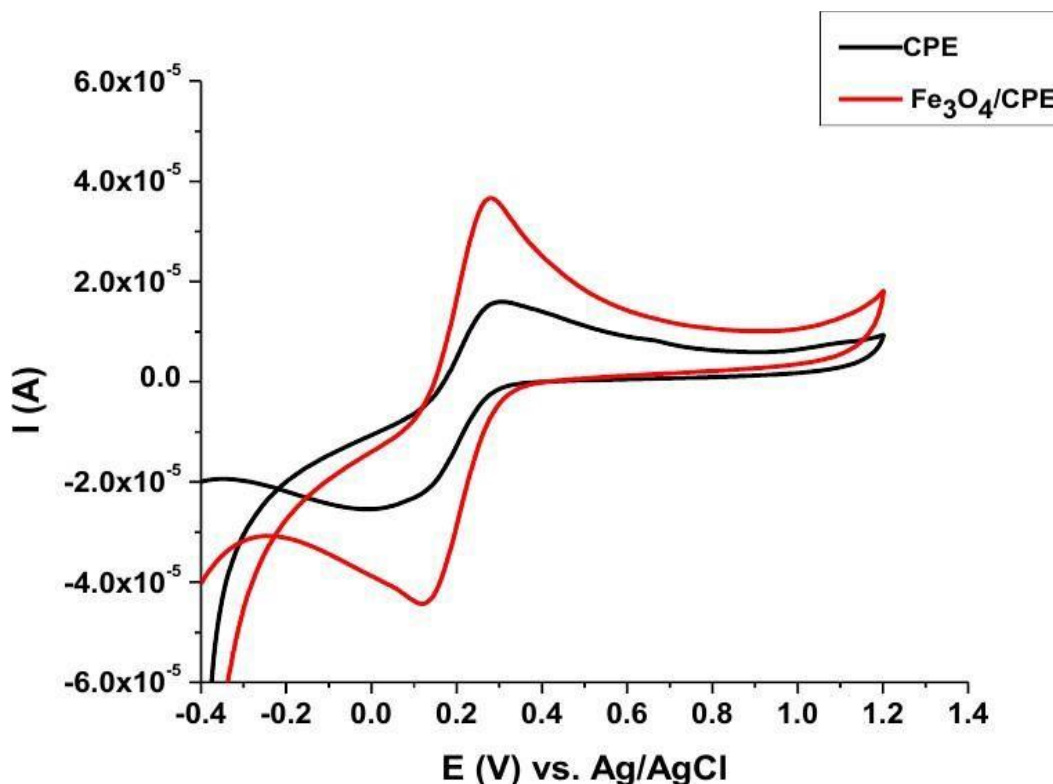
**Figure 5.1:** CV measurement of 2mM $K_3Fe(CN)_6$ at (a) CPE; and (b) $Fe_3O_4$ nanoparticles modified CPE, at 100 mV/s of the scan rate.

## 5.2. Effect of Different Concentrations of Potassium Ferricyanide

Figure 5.2 demonstrates the effect of the different concentrations of $K_3Fe(CN)_6$ on the oxidation/reduction signal current at the $Fe_3O_4$ nanoparticles modified CPE in 0.1 M $KNO_3$ solution. We can observe both the oxidation and reduction signal currents increased linearly with increasing concentration of $K_3Fe(CN)_6$ in the extent from 2 mM to 10 mM. Calibration curves behaviour linear relationships of $Ipa = 3\times10^{-6}\,C - 2\times10^{-7}$, ($R^2 = 0.9898$; N = 20) for oxidation signal current and $Ipc = -4\times10^{-6}\,C - 2\times10^{-7}$, ($R^2 = 0.9966$; N = 20) for reduction signal current, The LOD was determined by the mathematical formula $LOD = 3\times SD/m$ (whereas SD is the standard deviation of five measurements, while m is the slope obtained from the graph). For various concentrations of $K_3Fe(CN)_6$ (2 mM to 10 mM), $SD = 3.46\times10^{-7}$, and $m = 3\times10^{-6}$. Thedetection limit of $K_3Fe(CN)_6$ (oxidation process) was calculated as 0.38 mM.

41

**Figure 5.2:** The calibration CV curves of current versus concentration of (2, 4, 6, 8, 10 mM) $K_3Fe(CN)_6$. at $Fe_3O_4$ nanoparticles modified CPE.
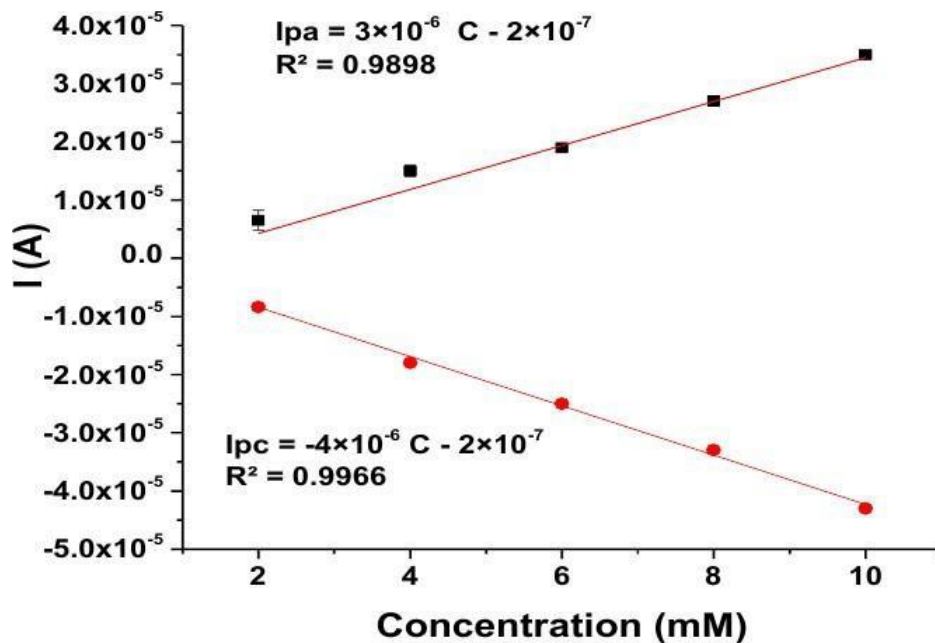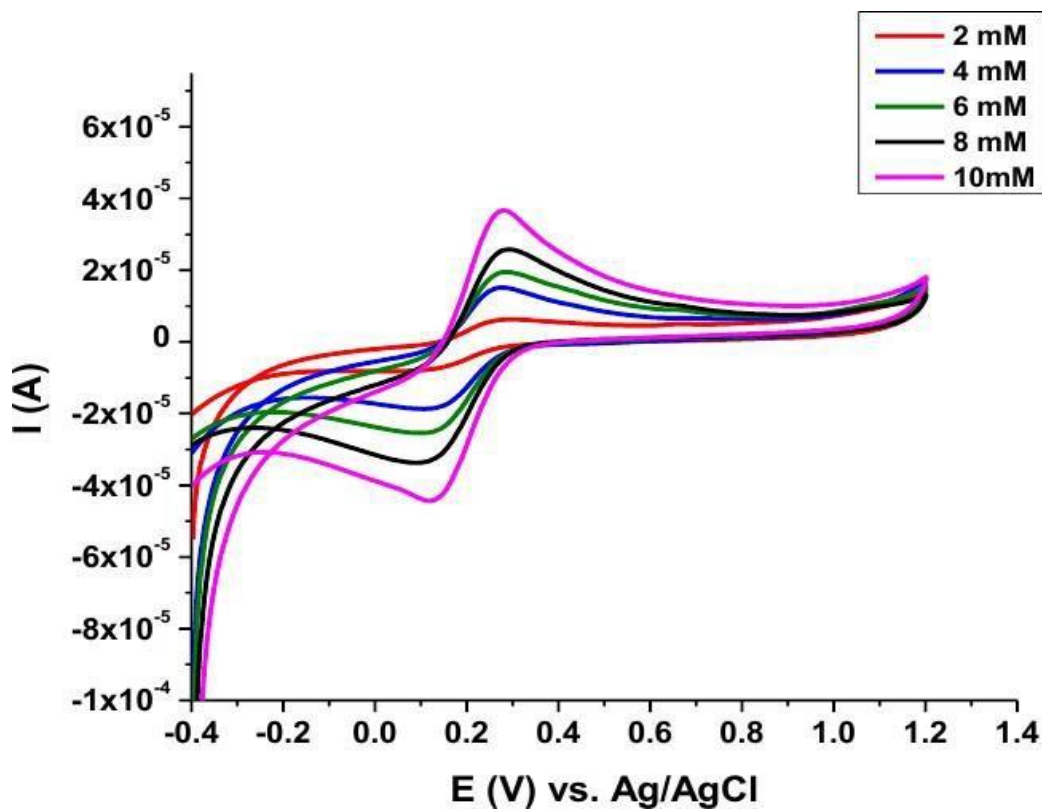


**Figure 5.3:** CV measurements of 2, 4, 6, 8, 10 mM at $Fe_3O_4$ nanoparticles modified CPE, at 100 mV/s of the scan rate.

## 5.3. Concentration study of Potassium Ferricyanide

To study different concentrations of $K_3Fe(CN)_6$ , at $Fe_3O_4$ nanoparticles modified CPE, it is observed that the peak-to-peak separation values in the range between 0.129V to 0.171 V with a mean of 0.151 V and standard deviation ±0.01792. We found from Table 1 that the height anodic/cathodic peaks current of $K_3Fe(CN)_6$ increased with a rise in the concentration from 2 mM to 10 mM.

**Table5. 1** Peak currents at various concentrations $K_3Fe (CN)_6$ at a scan rate of 100 mV/s.

| Concentration mM | Epa (V) | Epc (V) | Ipa (A) | Ipc (A) | ΔE (V) |
|---|---|---|---|---|---|
| 2 | 0.262 | 0.133 | $6.5×10^{-6}$ | $-6.6×10^{-6}$ | 0.129 |
| 4 | 0.267 | 0.128 | $1.6×10^{-5}$ | $-1.8×10^{-5}$ | 0.139 |
| 6 | 0.272 | 0.119 | $1.9×10^{-5}$ | $-2.5×10^{-5}$ | 0.153 |
| 8 | 0.276 | 0.109 | $2.6×10^{-5}$ | $-3.4×10^{-5}$ | 0.167 |
| 10 | 0.285 | 0.114 | $3.7×10^{-5}$ | $-4.4×10^{-5}$ | 0.171 |

## 5.4. Effect of Scan Rate

The Scanning Rate impact CV at various scanning rates. Impact on the strength of the peak current when diffusion or adsorption controls the redox process. The deformation process can be regarded proportional to the scan speed when Current peak is equal to The current density square root (linearly). Scans, pH, temperature and potassium ferricyanide levels at increased scanning rate were a significant factor in electrochemical reactions; peak current separation increased and peak potentials slightly shifted to positive and cathode levels in the direction of low temperatures as the anodic peak.Scan rate, as shown in Figure 5.4 the current increases approximately in a linear approach.
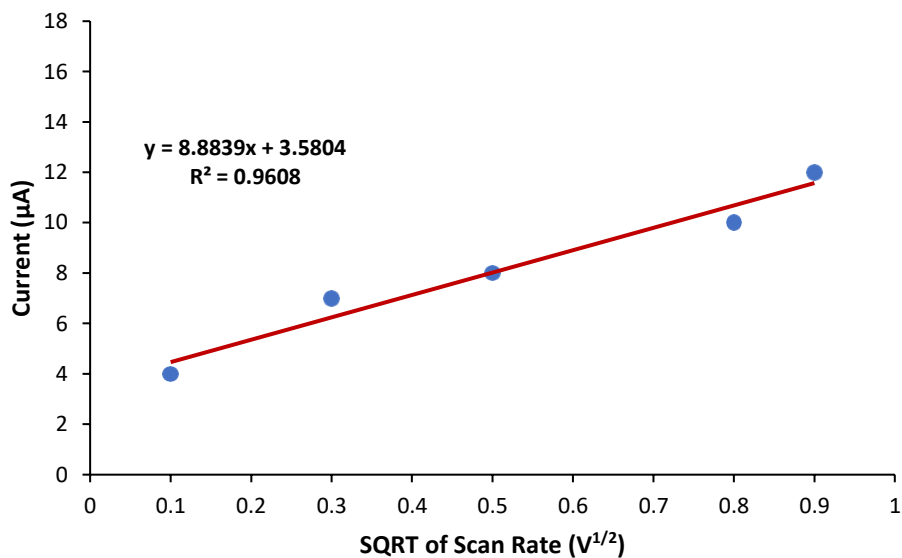
**Figure 5.4:** Effect of variation of scan rates of compound $K_3Fe(CN)_6$ by CPE NPs cyclic voltametric techniques.
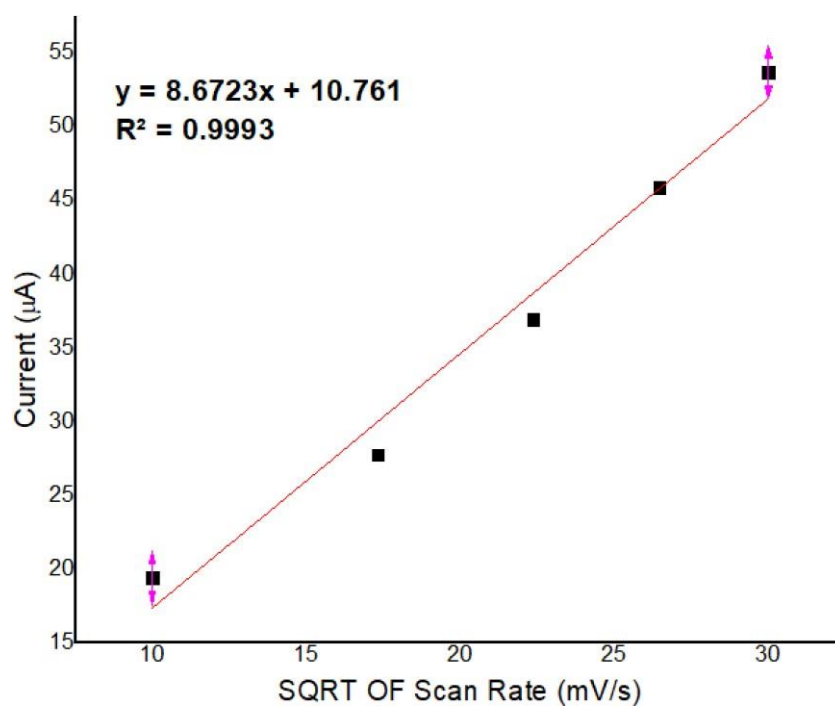


**Figure 5.5:** Effect of variation of scan rates of compound $K_3Fe(CN)_6$ by cyclic voltametric techniques at $Fe_3O_4$ nanoparticles unmodified CPE

In addition, various scan rate (100,300,500,700,900) was applying to the five concentrations (2, 4, 6, 8, 10), and the change of current was evident. tables those tables indicate the relation between the cathodic current and the anodic current for the redox reaction of potassium ferricyanide for the five-concentration used in order to prove the type of the redox reaction is the reversible reaction according to the ratio ipa/ipc approximately one as shown in table below that indicates the values around one.

**Table5. 2: Cyclic voltammetry data of compound 2mM in $K_3Fe(CN)_6$ at the different scan speed**

| Scan Rate (mVs$^{-1}$) | $E_{pc}$(V) | $E_{pa}$(V) | $\Delta E_p$(V) | $I_{pc}$(A) | $I_{pa}$(A) | $i_{pa}/i_{pc}$ |
|---|---|---|---|---|---|---|
| 100 | 0.5020 | 0.0043 | 0.4977 | $3.00*10^{-5}$ | $4.99*10^{-5}$ | 1.66 |
| 300 | 0.5462 | 0.0123 | 0.5339 | $3.102*10^{-5}$ | $4.00*10^{-5}$ | 1.28 |
| 500 | 0.4341 | 0.0242 | 0.4099 | $4.22*10^{-5}$ | $5.11*10^{-5}$ | 1.21 |
| 700 | 0.4221 | 0.0331 | 0.389 | $3.99*10^{-5}$ | $4.18*10^{-5}$ | 1.04 |
| 900 | 0.5628 | 0.0263 | 0.5365 | $2.11*10^{-5}$ | $3.08*10^{-5}$ | 1.45 |

**Table5. 3** Cyclic voltammetry data of compound 4mM in $K_3Fe(CN)_6$ at the different scan rate

| Scan Rate (mVs$^{-1}$) | $E_{pc}$(V) | $E_{pa}$(V) | $\Delta E_p$(V) | $I_{pc}$(A) | $I_{pa}$(A) | $i_{pa}/i_{pc}$ |
|---|---|---|---|---|---|---|
| 100 | 0.5634 | 0.0444 | 0.519 | $4.02*10^{-5}$ | $5.95*10^{-5}$ | 1.4 |
| 300 | 0.4862 | 0.0371 | 0.4491 | $4.88*10^{-5}$ | $5.00*10^{-5}$ | 1.02 |
| 500 | 0.4992 | 0.0385 | 0.4607 | $3.67*10^{-5}$ | $4.00*10^{-5}$ | 1.08 |
| 700 | 0.5229 | 0.0226 | 0.5003 | $3.861*10^{-5}$ | $4.22*10^{-5}$ | 1.09 |
| 900 | 0.5110 | 0.0118 | 0.4992 | $4.01*10^{-5}$ | $5.26*10^{-5}$ | 1.31 |

**Table5. 4: Cyclic voltammetry data of compound 6mM in $K_3Fe(CN)_6$ at the different scan speed**

| Scan Rate (mVs$^{-1}$) | $E_{pc}$(V) | $E_{pa}$(V) | $\Delta E_p$(V) | $I_{pc}$(A) | $I_{pa}$(A) | $i_{pa}/i_{pc}$ |
|---|---|---|---|---|---|---|
| 100 | 0.5356 | 0.0070 | 0.5286 | $4.10*10^{-5}$ | $5.65*10^{-5}$ | 1.3 |
| 300 | 0.5112 | 0.0289 | 0.4823 | $4.11*10^{-5}$ | $5.21*10^{-5}$ | 1.2 |
| 500 | 0.5004 | 0.0021 | 0.4983 | $3.92*10^{-5}$ | $4.91*10^{-5}$ | 1.2 |
| 700 | 0.4998 | 0.0231 | 0.4767 | $4.02*10^{-5}$ | $5.61*10^{-5}$ | 1.3 |
| 900 | 0.5334 | 0.0092 | 0.5242 | $3.22*10^{-5}$ | $4.18*10^{-5}$ | 1.2 |

**Table5. 5** Cyclic voltammetry data of compound 8mM in $K_3Fe (CN)_6$ at the different scan rate

| Scan Rate (mVs$^{-1}$) | $E_{pc}$(V) | $E_{pa}$(V) | $\Delta E_p$(V) | $I_{pc}$(A) | $I_{pa}$(A) | $i_{pa}/i_{pc}$ |
|---|---|---|---|---|---|---|
| 100 | 0.4593 | 0.0491 | 0.4102 | $1.72*10^{-5}$ | $3.19*10^{-5}$ | 1.85 |
| 300 | 0.4203 | 0.0521 | 0.3682 | $1.92*10^{-5}$ | $3.22*10^{-5}$ | 1.67 |
| 500 | 0.5181 | 0.0233 | 0.4948 | $2.86*10^{-5}$ | $3.00*10^{-5}$ | 1.56 |
| 700 | 0.4913 | 0.0329 | 0.4584 | $195*10^{-5}$ | $2.98*10^{-5}$ | 1.48 |
| 900 | 0.5201 | 0.0437 | 0.4764 | $2.00*10^{-5}$ | $3.40*10^{-5}$ | 1.7 |

**Table5. 6: Cyclic voltammetry data of compound 10mM in K₃Fe(CN)₆ at the different scan speed**

| Scan Rate (mVs⁻¹) | $E_{pc}(V)$ | $E_{pa}(V)$ | $\Delta E_p(V)$ | $I_{pc}(A)$ | $I_{pa}(A)$ | $i_{pa}/i_{pc}$ |
|---|---|---|---|---|---|---|
| 100 | 0.4610 | 0.1084 | 0.3526 | $2.57*10^{-6}$ | $6.7*10^{-5}$ | 2.6 |
| 300 | 0.4258 | 0.1021 | 0.3237 | $2.31*10^{-6}$ | $6.1*10^{-5}$ | 2.6 |
| 500 | 0.4823 | 0.1903 | 0.2920 | $2.84*10^{-6}$ | $6.0*10^{-5}$ | 2.1 |
| 700 | 0.4667 | 0.1281 | 0.3386 | $3.0*10^{-6}$ | $5.9*10^{-5}$ | 1.9 |
| 900 | 0.5031 | 0.1004 | 0.4027 | $2.51*10^{-6}$ | $6.45*10^{-5}$ | 2.5 |

those tables indicate the relation between the cathodic current and the anodic current for the redox reaction of potassium ferricyanide for the five concentration used in order to prove the type of the redox reaction is the reversible reaction according to the ratio $i_{pa}/i_{pc}$ approximately one as shown in table below that indicates the values more than 2 that indicate to only analyte without nanoparticles electrode surface area not smooth enough and those values without nanoparticles less sensitivity and less selectivity.

**Table5. 7: Cyclic voltammetry data of compound 2mM in K₃Fe(CN)₆ at the different sca rate Fe₃O₄ nanoparticles unmodified CPE**

| Scan Rate (mVs⁻¹) | $E_{pc}(V)$ | $E_{pa}(V)$ | $\Delta E_p(V)$ | $I_{pc}(A)$ | $I_{pa}(A)$ | $i_{pa}/i_{pc}$ |
|---|---|---|---|---|---|---|
| 100 | 0.5102 | 0.0376 | 0.4726 | $4.47*10^{-5}$ | $5.99*10^{-5}$ | 1.3 |
| 300 | 0.4861 | 0.0289 | 0.4563 | $4.00*10^{-5}$ | $5.78*10^{-5}$ | 1.44 |
| 500 | 0.4423 | 0.0310 | 0.4113 | $5.10*10^{-5}$ | $6.22*10^{-5}$ | 1.21 |
| 700 | 0.5286 | 0.0399 | 0.4887 | $4.08*10^{-5}$ | $5,00*10^{-5}$ | 1.2 |
| 900 | 0.5002 | 0.0410 | 0.4392 | $5.29*10^{-5}$ | $6.01*10^{-5}$ | 1.1 |

**Table5. 8**: **Cyclic voltammetry data of compound 4mM in $K_3Fe(CN)_6$ at the different scan rate $Fe_3O_4$ nanoparticles unmodified C PE**

| Scan Rate (mVs$^{-1}$) | $E_{pc}$(V) | $E_{pa}$(V) | $\Delta E_p$(V) | $I_{pc}$(A) | $I_{pa}$(A) | $i_{pa}/i_{pc}$ |
|---|---|---|---|---|---|---|
| 100 | 0.4463 | 0.0980 | 0.3483 | $1.35*10^{-6}$ | $3.6*10^{-6}$ | 2.6 |
| 300 | 0.4825 | 0.0983 | 0.3842 | $1.49*10^{-6}$ | $3.1*10^{-6}$ | 2.0 |
| 500 | 0.5103 | 0.0785 | 0.4318 | $2.0*10^{-6}$ | $3.9*10^{-6}$ | 1.9 |
| 700 | 0.4997 | 0.0891 | 0.4106 | $1.30*10^{-6}$ | $3.3*10^{-6}$ | 2.5 |
| 900 | 0.5223 | 0.0823 | 0.440 | $2.01*10^{-6}$ | $4.02*10^{-6}$ | 2.0 |

**Table5. 9: Cyclic voltammetry data of compound 6mM in $K_3Fe(CN)_6$ at the different scan rate $Fe_3O_4$ nanoparticles unmodified CPE**

| Scan Rate (mVs$^{-1}$) | $E_{pc}$(V) | $E_{pa}$(V) | $\Delta E_p$(V) | $I_{pc}$(A) | $I_{pa}$(A) | $i_{pa}/i_{pc}$ |
|---|---|---|---|---|---|---|
| 100 | 0.4540 | 0.0820 | 0.3720 | $1.03*10^{-6}$ | $2.98*10^{-6}$ | 2.8 |
| 300 | 0.4481 | 0.0912 | 0.3569 | $1.25*10^{-6}$ | $2.99*10^{-6}$ | 2.3 |
| 500 | 0.5102 | 0.0873 | 0.4229 | $1.99*10^{-6}$ | $3.9*10^{-6}$ | 1.9 |
| 700 | 0.4891 | 0.0902 | 0.3989 | $1.02*10^{-6}$ | $2.61*10^{-6}$ | 2.5 |
| 900 | 0.4770 | 0.0885 | 0.3885 | $2.0*10^{-6}$ | $4.10*10^{-6}$ | 2.0 |

**Table5. 10: Cyclic voltammetry data of compound 8mM in K$_3$Fe(CN)$_6$ at the different scan rate Fe$_3$O$_4$ nanoparticles unmodified C PE**

| Scan Rate (mVs$^{-1}$) | E$_{pc}$(V) | E$_{pa}$(V) | ΔE$_p$(V) | I$_{pc}$(A) | I$_{pa}$(A) | i$_{pa}$/i$_{pc}$ |
|---|---|---|---|---|---|---|
| 100 | 0.4451 | 0.0415 | 0.4036 | 4.24*10$^{-6}$ | 8.80*10$^{-6}$ | 2.0 |
| 300 | 0.4873 | 0.0481 | 0.4392 | 3.72*10$^{-6}$ | 7.50*10$^{-6}$ | 2.0 |
| 500 | 0.4981 | 0.0303 | 0.4678 | 4.51*10$^{-6}$ | 8.91*10$^{-6}$ | 1.9 |
| 700 | 0.4883 | 0.0379 | 0.4504 | 4.20*10$^{-6}$ | 8.6*10$^{-6}$ | 2.0 |
| 900 | 0.5331 | 0.0397 | 0.4934 | 3.91*10$^{-6}$ | 7.40*10$^{-6}$ | 1.9 |

**Table5. 11** Cyclic voltammetry data of compound 10mM in K$_3$Fe(CN)$_6$ at the different scan rate Fe$_3$O$_4$ nanoparticles unmodified CPE

| Scan Rate (mVs$^{-1}$) | E$_{pc}$(V) | E$_{pa}$(V) | ΔE$_p$(V) | I$_{pc}$(A) | I$_{pa}$(A) | i$_{pa}$/i$_{pc}$ |
|---|---|---|---|---|---|---|
| 100 | 0.3951 | 0.0169 | 0.3782 | 1.82*10$^{-5}$ | 2.93*10$^{-5}$ | 1.6 |
| 300 | 0.4101 | 0.0119 | 0.4563 | 2.00*10$^{-5}$ | 3.6*10$^{-5}$ | 1.8 |
| 500 | 0.4218 | 0.0210 | 0.4113 | 2.10*10$^{-5}$ | 3.8*10$^{-5}$ | 1.8 |
| 700 | 0.4003 | 0.0199 | 0.4887 | 1.98*10$^{-5}$ | 2.9*10$^{-5}$ | 1.4 |
| 900 | 0.4832 | 0.03810 | 0.4392 | 2.29*10$^{-5}$ | 3.31*10$^{-5}$ | 1.4 |

For the cyclic voltammetry method which indicate a reversible reaction for a reduces reaction and this can seen in table 5.12 for a reversible reaction the potential of the cathodic peak should be almost similar in height for the potential anodic peak hence the different between the two potential of the cathodic and anodic peaks should be approximately one some date shown in table below were taken manually by using origin program for more prices results to be for the five concentration the value (ΔEp) close to one which indicates reversible reaction.

**Table5. 12** Cyclic voltammetry manual data of compounds 2,4,6, 8,10mM in $K_3Fe\,(CN)_6$

| Concentration Mm | $E_{pc}(V)$ | $E_{pa}(V)$ | $\Delta E_p(V)$ | $i_{pc}(A)$ | $i_{pa}(A)$ | $i_{pa}/i_{pc}$ |
|---|---|---|---|---|---|---|
| 2 | 0.2966 | 0.16739 | 0.1292 | $4.1167*10^{-6}$ | $5.115*10^{-6}$ | 1.24 |
| 4 | 0.2651 | 0.15367 | 0.1114 | $1.7136*10^{-5}$ | $1.9357*10^{-5}$ | 1.12 |
| 6 | 0.2939 | 0.1615 | 0.1324 | $2.00*10^{-5}$ | $2.349*10^{-5}$ | 1.17 |
| 8 | 0.2907 | 0.1167 | 0.174 | $2.709*10^{-5}$ | $3.285*10^{-5}$ | 1.21 |
| 10 | 0.2829 | 0.1416 | 0.1413 | $3.9067*10^{-5}$ | $4.2813*10^{-5}$ | 1.09 |

### 5.5 : Diffusion coefficient

In linear sweep Voltammetry (LSV) and cyclic voltammetry, single electrical approaches are widespread utilized to measure the coefficient or diagnosis of the analyte or to assess the electro-chemical surface (radius) of the working electrode (CV). The present vs. tensility curves can be either logarithmic, equation 1 or peak shaped, and in experimental investigations the steady state peak (IP) curves can give significant analytical information, depending on the experimental conditions (mass media viscosity, molecular analyte mass, range of scans, etc.).

We assume that the surface of the electrode is smooth, so r =0.4 cm Hence, the surface area A of the electrode can be calculated by:

$$A = \pi r^2$$
$$= (3.14)\,(0.4)^2$$
$$A = 0.5029 \text{ cm}^2$$

By the substitution of A in Fick's law, D can found:Ip

$$= (2.69 \times 10^5)\, n^{1/2}\, D^{1/2}\, ACv^{1/2}$$
$$5*10^{-5}\,(A){=}2.69*10^5 * (1)^{3/2} *(0.5029) \text{ cm}^2 *D^{1/2} *2*10^{-3}(mol/cm^3)$$
$$D= 3.4151*10^{-10} \text{ cm}^2/s$$

The surface area A of the electrode CPE NPs can be

calculated byIp $= (2.69 \times 10^5)\, n^{1/2}\, D^{1/2}\, ACv^{1/2}$

$$2.0*10^{-5}A = 2.69*10^5 * (1)^{3/2} *A*3.4151*10^{-10}cm^2/s *$$

$$2*10^{-3}(mol/cm^3)A = 1.08*10^2 \, cm^2$$

So the surface area A increase with the carbon paste electrode NPs.

For disc-shaped working electrodes, the equations of Ip to experimental conditions are:

$$Ip = 4nFDCr \hspace{4cm} \text{Eq. 1}$$

$$Ip = (2.69 \times 10^5) \, n^{3/2} D^{1/2} \, ACv^{1/2} \hspace{2.5cm} \text{Eq. 2}$$

IP(A) means recorded peak currents, F is Faraday, D (cm2/s) is a diffusion coefficient, A(cm2) is a surface area and r is an electrode's radius, v is the scanning rate and C (mol/cm3) is the analyser's concentration. In addition to Nicholson and Shain, Fick's solutions for the distribution of a disk electrode embedded in an electro-reversible redox process have been presented and (Sheppard et al., 2017).

Linear regression equation expressed

as

$$I_{pa} = 2.69*10^5 n^{3/2}AD^{1/2}C_0V^{1/2}$$

The above result the process is diffusion controlled.


## 5.6 : Differential Pulse Voltammetry

Differential pulse voltammetry (DPV) is a SWV similar voltammetric technique with an increased discrimination against Faradaic currents (electron transmission to and from an electrode) obtainable using DPV, DPV can also offer an increased selection for observing various redox processes resulting from an increasing pult current and the connection between concentration and current is advantageous. Figure 5.6 illustrated the behavior of potassium ferricyanide, which varied from 2 mM to 10 Mm when differential pulses were delivered risingin maximum height.
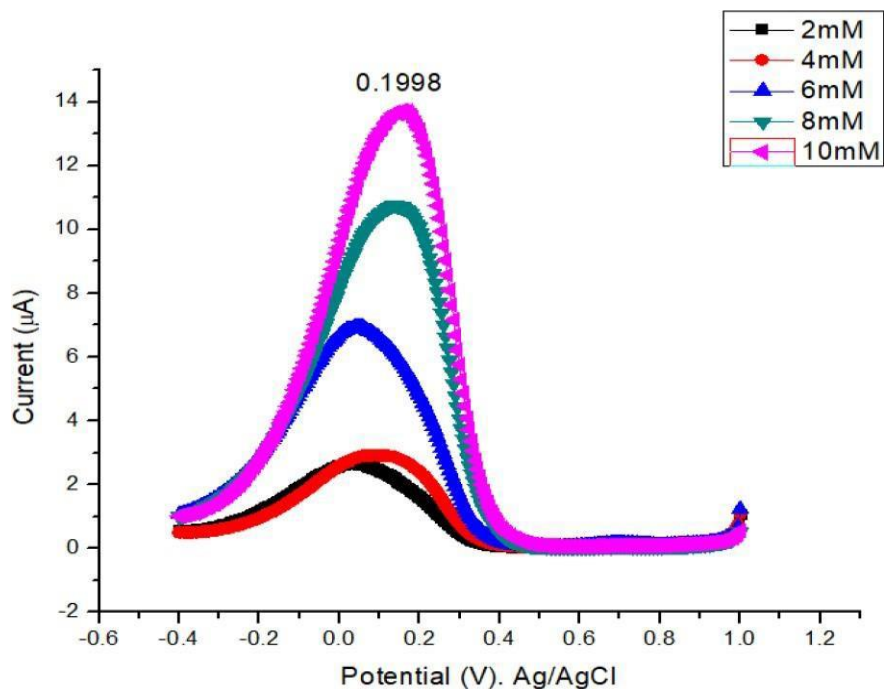
**Figure 5.6:** Differential pulse voltammetry DPV measurement of concentration of 2, 4, 6, 8, 10 $K_3Fe(CN)_6$. at $Fe_3O_4$ nanoparticles unmodified CPE.

To increase the sensitivity of the voltammogram output iron oxide, NPs were added in an appropriate amount to the CPE to detect the same five different concentration of ferricyanide mentioned before. Figure 5.6 shows the difference between two peak related to the same concentration but in different peak height peak without the addition of NPs to the CPE and the second when NPs were added, indicating the highest one.
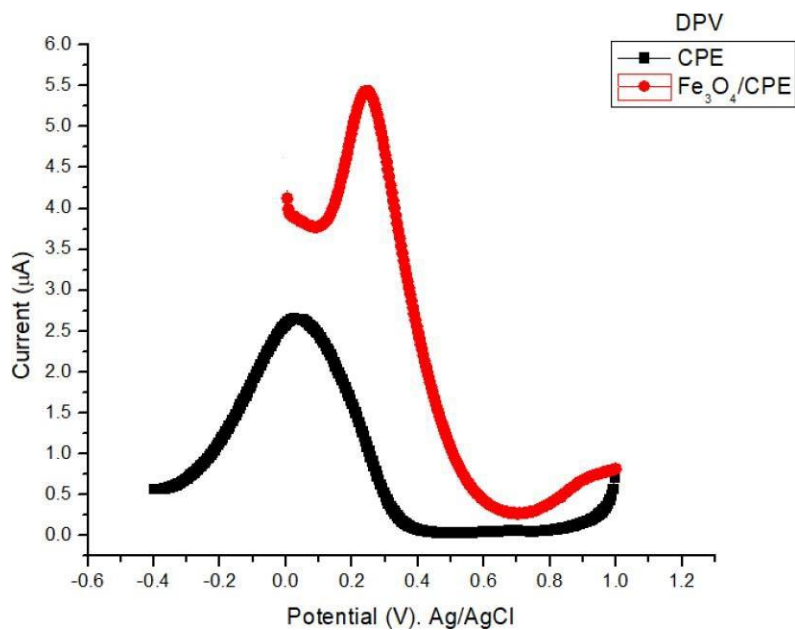
**Figure 5.7:** DPV measurement of 2mM $K_3Fe(CN)_6$ at (a) CPE; and (b) $Fe_3O_4$ nanoparticles modified CPE
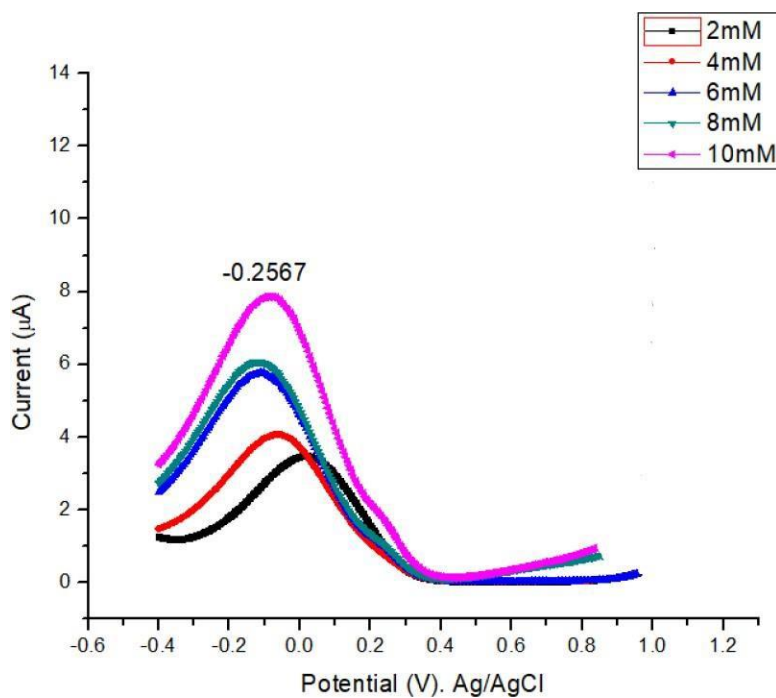


**Figure 5.8:** DPV measurements of 2, 4, 6, 8, 10 mM at $Fe_3O_4$ nanoparticles modified

Figure 5.9 demonstrates the effect of the different $K_3Fe(CN)_6$ the signal current at the $Fe_3O_4$ nanoparticles modified CPE in a 0.1 M $KNO_3$ solution. can observe the signal currents increased linearly with increasing concentration of $K_3Fe(CN)_6$ in the extent from 2 mM to 10 mM. Calibration curves behavior linear relationships of (Ip=0.0565x C-0.0034 and $R^2$=0.9932).
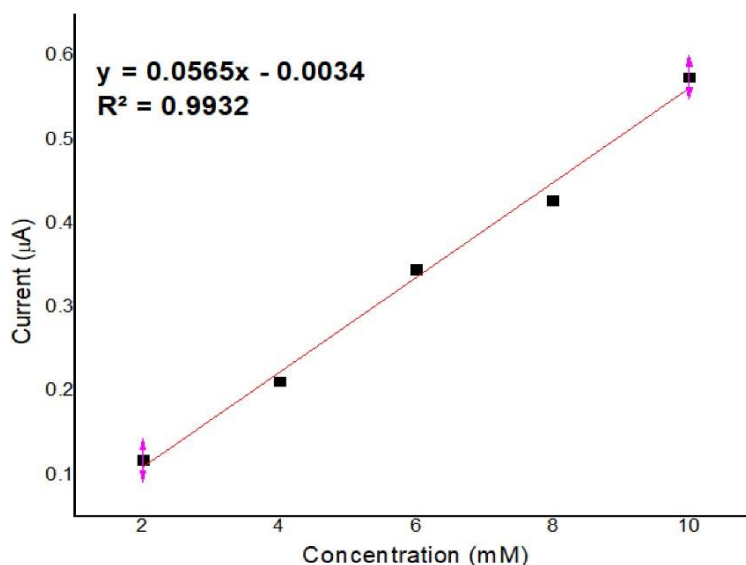


**Figure 5.9:** The DPV calibration curve of various concentrations of (2, 4, 6, 8, 10 mM) at $Fe_3O_4$ nanoparticles modified CPE

### 5.7: Square wave voltammetry

Voltammetry Square-Wave (SWV) is an electro-chemical compassionate technique used to detect devices based on the idea of an increased signal-to-noise ratio by the square root of the scan rate. This signal enhancement depends on the duration between pulse applications. Due to its great sensitivity and selectivity, SWV measuring technology was also utilized to build sensors and biosensors, resulting in a marked rise of the peak current. The authors noted that the peak current had a linear dependency on analytes.By applying different potential pulses to the five different concentrations 2, 4, 6, 8, 10 mM, extra peak height observed in the voltammogram obtained, the increase in concentration potassium ferricyanide the current also increased due to the electron transfer by the redox reaction as can be shown in figure 5.10.
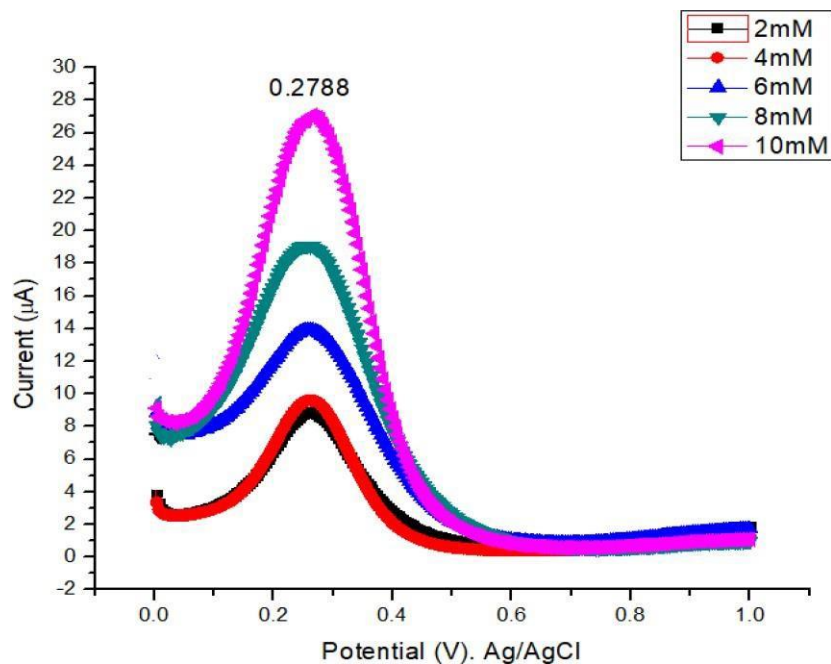
**Figure 5.10:** Square wave voltammetry SWV measurement of the concentration of (2, 4, 6, 8, 10) mM $K_3Fe(CN)_6$ at $Fe_3O_4$ nanoparticles unmodified CPE.

The mixing of iron oxide NPs with the CPE enhances the electrode's surface area; hence, the reaction rate will increase. So, the difference in peak height can be described in figure 5.11 related to the same concentration of ferricyanide. The peak which has the lowest peak height indicates the usage of CPE without iron oxide NPs.
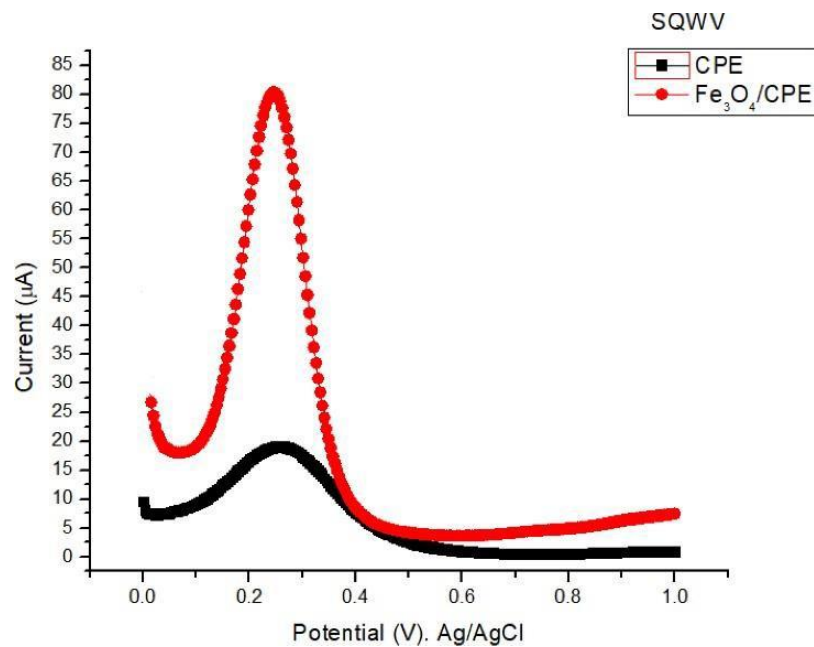
**Figure 5.11:** SWV measurement of 8mM $K_3Fe(CN)_6$ at (a) CPE; and (b) $Fe_3O_4$ nanoparticles modified CPE

The addition of iron oxide NPs to the CPE helps increase the rate of electron transfer; thus, the current will also be increased. This relation clearly can be seen in figure 5.12 below for the five different concentrations started from the lowest concentration till the highest one.
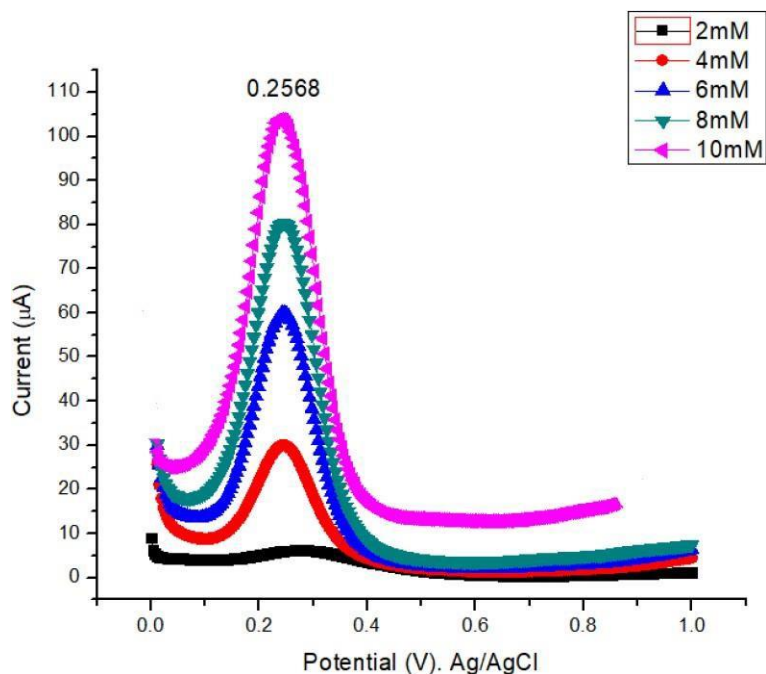
**Figure 5.12:** SWV measurements of 2, 4, 6, 8, 10 mM at $Fe_3O_4$ nanoparticles modified CPE.

Figure 5.13 demonstrates the effect of the different $K_3Fe(CN)_6$ the signal current at the $Fe_3O_4$ nanoparticles modified CPE in a 0.1 M $KNO_3$ solution. We can observe the signal currents increased linearly with increasing concentration of $K_3Fe(CN)_6$ in the extent from 2 mM to 10 mM. Calibration curves behavior linear relationships of (Ip=0.5489x C+0.2717 and $R^2$=0.9937)
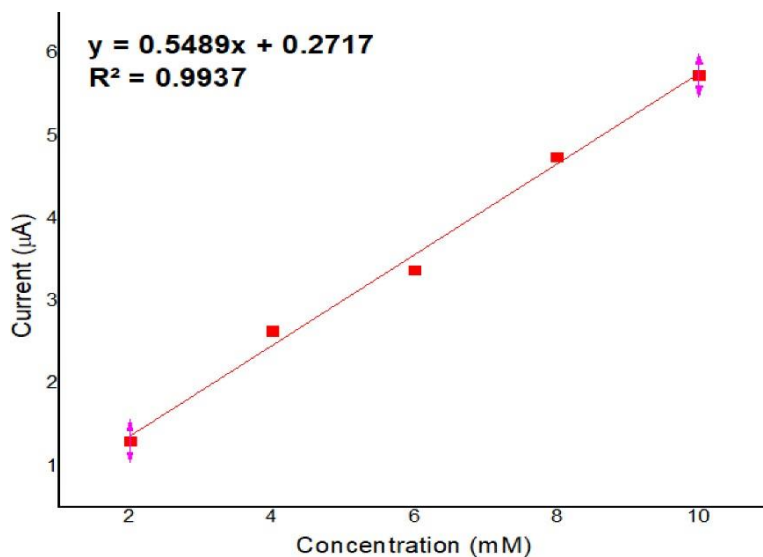
**Figure 5.13:** The SWV calibration curves of various concentrations of $K_3Fe(CN)_6$ (2, 4, 6, 8, 10 mM) Vs. Current. at $Fe_3O_4$ nanoparticles modified CPE.

## 5.8 : Comparison among CV, DPV, SWV

SWV has more sensitivity more that DPV and CV due to the absence of the background current, which indicates an interference; on the other hand, DPV can be considered as a more straightforward technique than SWV because of the more complex data and specific details obtained, for instance, forward and backward current measurements which usually are ignored in most studies due to their complexity and cyclic voltammetry the anodic peak increase with the increase in analyte concentration.

**Table5. 13: Comparing between CV, DPV, SWV**

| Method | Sample | RSD(mM) | LOD (mM) | $R^2$ | Slope(A/mM) |
|--------|--------|---------|----------|-------|-------------|
| **CV** | Potassium Ferricyanide | $3.460*10^{-7}$ | 0.38 | 0.989 | $3*10^{-6}$ |
| **DPV** | Potassium Ferricyanide | $6.037*10^{-3}$ | 0.32 | 0.993 | 0.056 |
| **SWV** | potassium ferricyanide | $5.621*10^{-2}$ | 0.30 | 0.993 | 0.548 |

## 5.9 : Electrochemical Behavior of Potassium Ferricyanide Carried out using ML

The CV, DPV, SWV was performed in variable concentrations of $K_3Fe(CN)_6$ at each $Fe_3O_4$ nanoparticles modified CPE and unmodified CPE. Different measurements were acquired and analyzed to identify the processes related to the detected signals. Several figures were obtained for each concentration of $K_3Fe(CN)_6$ and each measurement provides the redox process potential voltage.

After analysis of the cyclic voltammetry data by the GBA technique, the outcomes showed that the ratio of the behavior of $K_3Fe(CN)_6$ at CPE was found 90% ,DPV 80% , SWV 80% While the proportion of $K_3Fe(CN)_6$ at $Fe_3O_4$ nanoparticles modified, CPE was found 97% ,DPV 75% ,SWV 82%.

DPV in the voltammograms with nanoparticles a shift to the left occurred which caused the potential value to be negative 0.2 instead of of positive 0.2 that's why the accuracy in ML is less with NPs.
Figure 5.14 indicates the classification of the five different concentration of potassium ferricyanide by GBA and 90% was achieved. On the other hand 97% was achieved for the data of nanoparticles added to the CPE as shown figures 5.15 which prove the higher accurse of classification achieved when NPs are used for the detection of the analyses.

### Table5. 14: Result of GBA

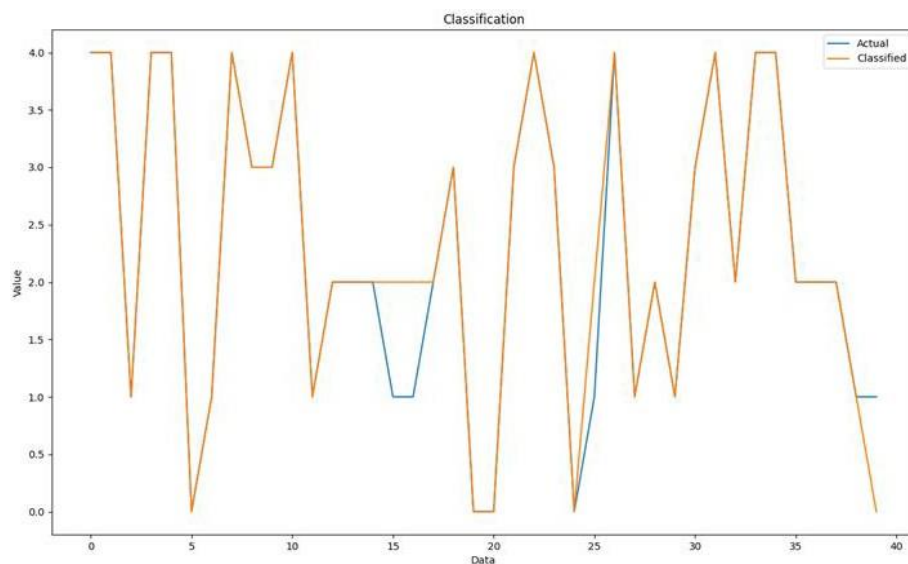| Method | + NPs | - NPs |
|--------|-------|-------|
| CV | 97% | 80% |
| DPV | 75% | 80% |
| SWV | 82% | 75% |

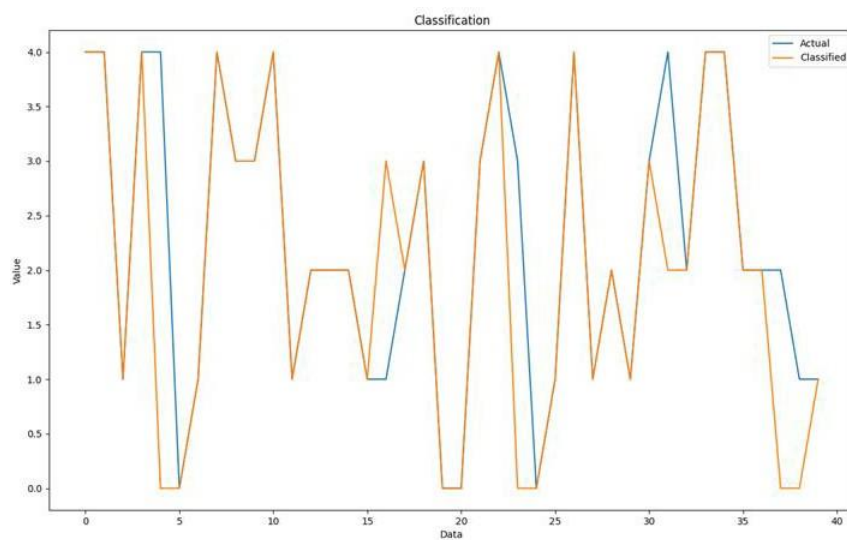**Figure 5.14:** CV, GBA of $K_3Fe(CN)_6$ at CPE



**Figure 5.15:** CV, GBA of $K_3Fe(CN)_6$ at $Fe_3O_4$ nanoparticles modified CPE

Figure 5.16 indicates the classification of the five different concentration of potassium ferricyanide by GBA and 80% was achieved. On the other hand, 75% was achieved for the data of nanoparticles added to the CPE as shown figures 5.17 which prove the higher accurse of classification achieved when NPs are used for the detection of the analyses. DPV in the voltammograms with nanoparticles a shift to the left occurred which caused the potential value to be negative 0.2 instead of positive 0.2 that's why the accuracy in ML is less with NPs.
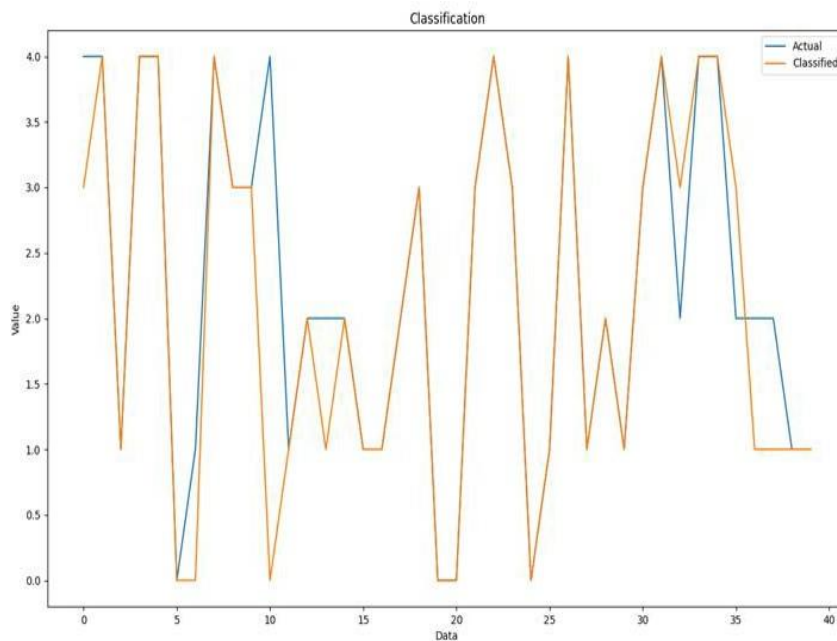


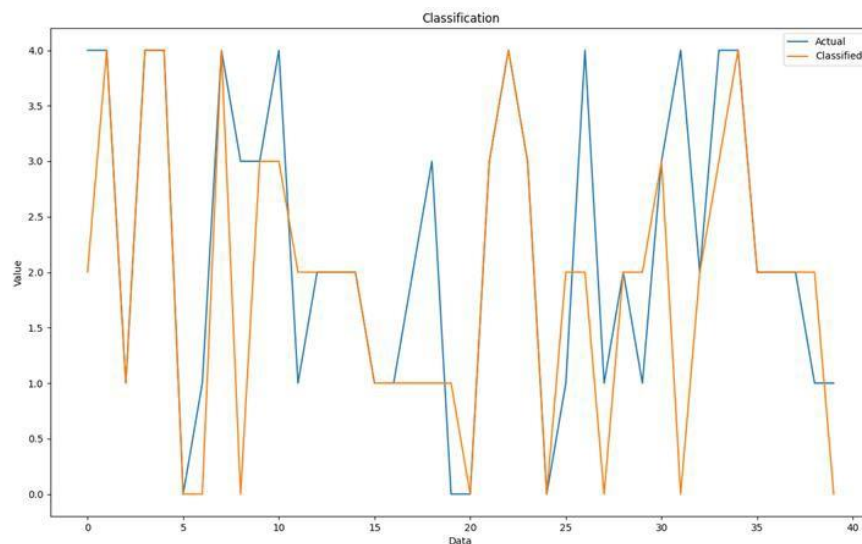**Figure 5.16:** DPV, GBA of $K_3Fe(CN)_6$ at CPE

**Figure 5.17:** DPV, GBA of $K_3Fe(CN)_6$ at $Fe_3O_4$ nanoparticles modified CPE

Figure 5.18 indicates the classification of the five different concentration of potassium ferricyanide by GBA and 80% was achieved. On the other hand 82% was achieved for the data of nanoparticles added to the CPE as shown figures 5.19 which prove the higher accurse of classification achieved when NPs are used for the detection of the analyses
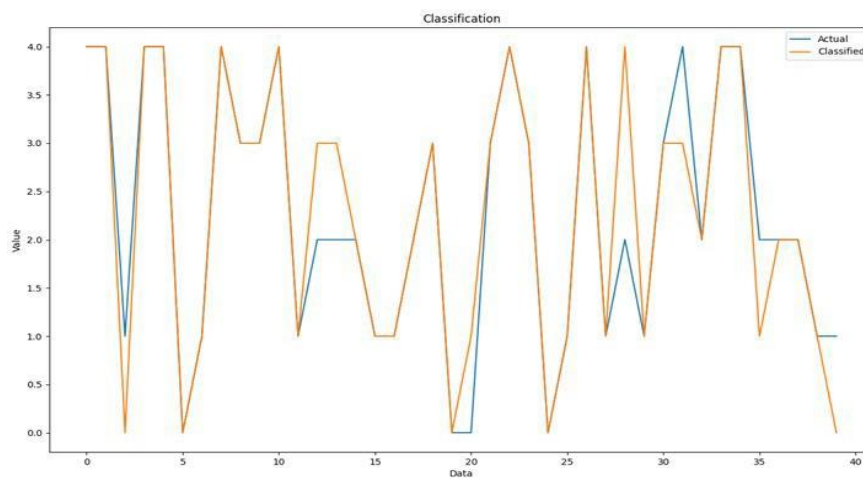


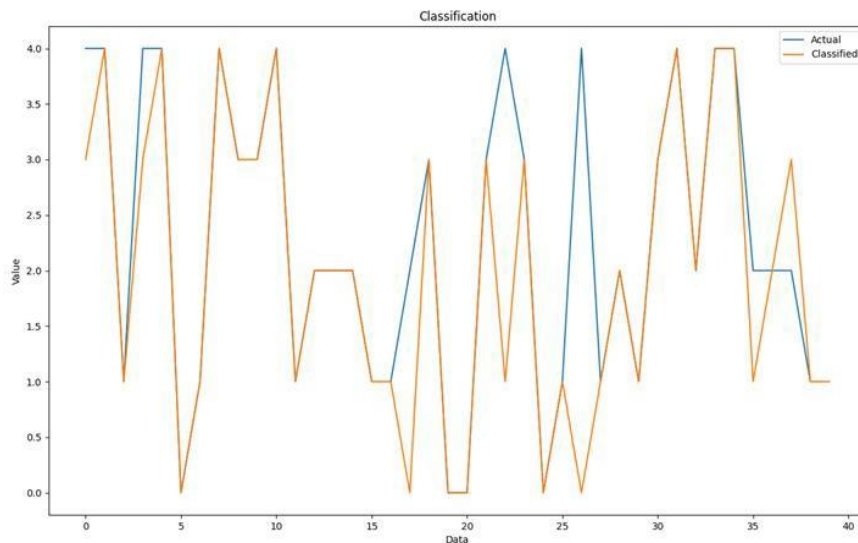**Figure 5.18:** SWV, GBA of $K_3Fe(CN)_6$ at CPE

**Figure 5.19:** SWV, GBA of $K_3Fe(CN)_6$ at $Fe_3O_4$ nanoparticles modified CPE

**table 5.15:** Table of merit for the electrochemical techniques used for the detection of potassium ferric cyanide

| Analyte | Technique | Linear range (µM) | Slope (A/mM) | Replicates | $R^2$ | RSD (mM) | LOD (mM) |
|---|---|---|---|---|---|---|---|
| Potassium Ferric Cyanide | CV | 2-10 | $3*10^{-6}$ | 20 | 0.989 | $\pm 3.460*10^{-7}$ | 0.38 |
| Potassium Ferric Cyanide | DPV | 2-10 | 0.056 | 20 | 0.993 | $\pm 6.037*10^{-3}$ | 0.32 |
| Potassium Ferric Cyanide | SWV | 2-10 | 0.548 | 20 | 0.993 | $\pm 5.621*10^{-2}$ | 0.30 |

# CHAPTER 6
## CONCLUSION

Potassium ferricyanide was investigated electrochemically using an improved carbon paste electrode with $Fe_3O_4$ nanoparticles. The outcome showed the use of the $Fe_3O_4$ nanoparticles modified CPE is highly signal current in the cyclic voltammetry measurement. Advances in nanotechnology intend new and innovative applications. therefore, there will be significant growth in future the application of nanotechnology because the major companies that have been active in nanomaterials. Applications of magnetic nanoparticles like Magnetic Resonance Imaging (MRI), drug delivery etc. Electrocatalytic response and sensitivity were enhanced when the $Fe_3O_4$ nanoparticles modified CPE was utilized compared to when unmodified CPE was used. The electrochemical techniques used in this study it can be concluded the differences in sensitivity among the voltametric techniques used in the detection of ferricyanide, this was clear in the value of the correlation coefficient founded, moreover the measurements of both LOD and LOQ which indicate the high selectivity and accuracy of the methods used, The reason for the increase in the signal in the cyclic voltammetry measurementis the high degree of electrical conductivity of the $Fe_3O_4$ nanoparticles; this is due to the presence of two oxidation states, which lead to an increase in the electron transferprocess. After analyzing the CV, DPV, SWV data by the GBA technique, Machine Learning techniques are widely used in various fields for classification purposes. A machine learning technique which is Gradient Boosting Function has been considered in order to classify the variants. the outcomes showed that the ratio of the behavior of $K_3Fe(CN)_6$ at CPE was found 90% for CV and 80% for DPV and 75% for SWV .In comparison, the rate of $K_3Fe(CN)_6$ at $Fe_3O_4$ nanoparticles modified CPE was found 97% for CV and 75% for DPV and 82% for SWV. Study results indicate that ML can analyze several data that allows the resolution of many redox reactions with high speed and accuracy in thedata analysis process; SWV has more sensitivity more that DPV due to the absence ofthe background current, while on the other hand, DPV can be considered as a more uncomplicated technique than SWV because of the more complex data and specific details obtained the surface area A is increased with iron oxide nanoparticles form 0.5029 to $1.08*10^2$ with NPs nanoparticles increase the surface area.

# REFERENCES

A. J. Bard and L. R. Faulkner, (2001). "Electrochemical Methods: Fundamentals and Applications," Wiley & Sons, inc., New York, (2001) pp. (87-162).

Ajay Kumar Gupta 1, Mona Gupta. (2005). Synthesis and Surface Engineering of Iron Oxide Nanoparticles for Biomedical Applications, 26(18):3995-4021.

Ali, M. H., Al-Maliki, A., El-Ali, B., Martinie, G., & Siddiqui, M. N. (2006). Deep desulphurization of gasoline and diesel fuels using non-hydrogen consuming techniques. Fuel, 85(10-11), 1354-1363.

Apetrei, I. M., & Apetrei, C. (2016). Application of voltammetric e-tongue for the detection of ammonia and putrescine in beef products. Sensors and Actuators B: Chemical, 234, 371-379.

Asir, S., Dimililer, K., Kirsal-Ever, Y., Özsöz, M., & Shama, N. A. (2019, October). Electrochemical Determination of Potassium Ferricyanide using Artificial Intelligence. In 2019 3rd International Symposium on Multidisciplinary Studies and Innovative Technologies (ISMSIT) (pp. 1-4). IEEE.

Bharde, A. A., Parikh, R. Y., Baidakova, M., Jouen, S., Hannoyer, B., Enoki, T., ... & Sastry, M. (2008). Bacteria-mediated precursor-dependent biosynthesis of superparamagnetic iron oxide and iron sulfide nanoparticles. Langmuir, 24(11), 5787-5794.

Chen, Y., Jia, Z., Mercola, D., & Xie, X. (2013). A gradient boosting algorithm for survival analysis via direct optimization of concordance index. Computational and mathematical methods in medicine, 2013.

Çubuku, M., Timur, S., & Anik, L. (2007). Examination of performance of glassy carbon paste electrode modified with gold nanoparticle and xanthine oxidase for xanthine and hypoxanthine detection. Talanta, 74(3), 434-439.

D. Salari, N. Daneshvar, F. Aghazadeh, A.R. Khataee, J. Hazard. Mater. 125 (2005) 205–210. [10] A. Niaei, J. Towfighi, A.R. Khataee, K. Rostamizadeh, Pet. Sci. Technol. 25 (2007) 967–982. [11] A. Aleboyeh, M.B. Kasiri, ME Olya,

H. Aleboyeh, Dyes Pigments 77 (2008) 288– 294.

Desmond C. C, Gilbert R. H., Hyperfine Interactions. 139/140 (2002) 597-606. Fazio, T. T., Singh, A. K., Kedor-Hackmann, E. R. M., & Santoro, M. I. R. M. (2007).

Quantitative determination and sampling of azathioprine residues for cleaning validation in the production area. Journal of pharmaceutical and biomedical analysis, 43(4), 1495-1498.

Galík, M., Cholota, M., Švancara, I., Bobrowski, A., & Vytřas, K. (2006). A study on stripping voltammetric determination of osmium (IV) at a carbon paste electrode modified in situ with cationic surfactants. Electroanalysis: An International Journal Devoted to Fundamental and Practical Aspects of Electroanalysis, 18(22), 2218-2224.

Ganchimeg Perenlei, Tan Wee Tee, Nor Azah Yusof, Goh Joo Kheng, Int. J. Electrochem. Sci. 6 (2011) 520 – 531.

Gupta, A. K., & Gupta, M. (2005). Synthesis and surface engineering of iron oxide nanoparticles for biomedical applications. Biomaterials, 26(18), 3995-4021.

He, K., Xu, C. Y., Zhen, L., & Shao, W. Z. (2007). Hydrothermal synthesis and characterization of single-crystalline Fe3O4 nanowires with high aspect ratio and uniformity. Materials Letters, 61(14-15), 3159-3162.

J. Guo and E. Lindner, J Electroanal Chem. 629 (2009) 180- 184.

J. Zupan, J. Gasteiger, Neural Networks for Chemists: An Introduction, VCH, Weinheim, 1993.

J.G. Vlasov, A.V. Legin, A.M. Rudnitskaya, A. d'Amico, C. Di Natale, J. Anal. Chem. 52 (1997) 1087.

Jia, C. J., Sun, L. D., Yan, Z. G., Pang, Y. C., You, L. P., & Yan, C. H. (2007). Iron

oxide tube-in-tube nanostructures. The Journal of Physical Chemistry C, 111(35), 13022-13027.

Kalcher, K., Schachl, K., Svancara, I., Vytras, K., & Alemu, H. (1999). Recent progress in the development of electrochemical carbon paste sensors. ChemInform, 30(1), no-no.

Klinkenberg, R., Streel, B., & Ceccato, A. (2003). Development and validation of a liquid chromatographic method for the determination of amlodipine residues on manufacturing equipment surfaces. Journal of pharmaceutical and biomedical analysis, 32(2), 345-352.

Kovalenko, M. V., Bodnarchuk, M. I., Lechner, R. T., Hesser, G., Schäffler, F., & Heiss, W. (2007). Fatty acid salts as stabilizers in size-and shape-controlled nanocrystal synthesis: the case of inverse spinel iron oxide. Journal of the American Chemical Society, 129(20), 6352-6353.

Kuwana, T., & French, W. G. (1964). Electrooxidation or Reduction of Organic Compounds into Aqueous Solutions Using Carbon Paste Electrode. Analytical Chemistry, 36(1), 241-242.

Laurent, S., Forge, D., Port, M., Roch, A., Robic, C., Vander Elst, L., & Muller, R. N. (2008). Magnetic iron oxide nanoparticles: synthesis, stabilization, vectorization, physicochemical characterizations, and biological applications. Chemical reviews, 108(6), 2064-2110.

Liu, Z., Zhang, D., Han, S., Li, C., Lei, B., Lu, W., ... & Zhou, C. (2005). Single crystalline magnetite nanotubes. Journal of the American Chemical Society, 127(1), 6-7.

M. Cho, et al., Nucleic Acids Research, 34 (2008) 75.

Morais, J. A., Zlotecki, R. A., Sakmar, E., Stetson, P. L., & Wagner, J. G. (1981). Specific and sensitive assays for digoxin in plasma, urine and heart tissue. Research communications in chemical pathology and pharmacology, 31(2), 285-298.

Niranjana, E., Swamy, B. K., Naik, R. R., Sherigara, B., & Jayadevappa, H., (2009) Journal of Electroanalytical Chemistry, 6311-9.

Pandurangachar, M., Swamy, B. K., Chandrashekar, B. N., Gilbert, O., Reddy, S., & Sherigara, B. S. (2010). Electrochemical investigations of potassium ferricyanide and dopamine by 1-butyl-4-methylpyridinium tetrafluoro borate modified carbon paste electrode: A cyclic voltammetric study. Int J Electrochem Sci, 5(8), 1187-1202.

Poole, Mackworth & Goebel (1998). Computational Intelligence, a logical approach, p. 1

Roh, Y., Vali, H., Phelps, T. J., & Moon, J. W. (2006). Extracellular synthesis of magnetite and metal-substituted magnetite nanoparticles. Journal of nanoscience and nanotechnology, 6(11), 3517-3520.

Russell & Norvig 2003, pp. 739–748, 758 and Luger & Stubblefield 2004, pp. 458 467. Feedforward neural networks, perceptrons and radial basis network.

S.N. Deming, S.L. Morgan, Experimental Design: A Chemometric Approach, Elsevier, Amsterdam, 1989.

Schultz, F. A., & Kuwana, T. (1965). Electrochemical studies of organic compounds dissolved in carbon-paste electrodes. Journal of Electroanalytical Chemistry (1959), 10(2), 95-103.

Shabani, R., Lakhaiy Rizi, Z., & Moosavi, R. (2018). Selective Potentiometric Sensor for Isoniazid Ultra-Trace Determination Based on Fe3O4 Nanoparticles Modified Carbon Paste Electrode (Fe3O4/CPE). International Journal of Nanoscience and Nanotechnology, 14(3), 241-249.

Shahrokhian, S., & Asadian, E. (2010). Simultaneous voltammetric determination of ascorbic acid, acetaminophen and isoniazid using thionine immobilized multi-walled carbon nanotube modified carbon paste electrode. Electrochimica Acta, 55(3), 666-672.

Sheppard, J. B., Hambly, B., Pendley, B., & Lindner, E. (2017). Voltammetric determination of diffusion coefficients in polymer membranes. Analyst, 142(6), 930-937.

Shi, S., Li, Z., Chen, H., & Zeng, F. (2008). Development and validation of an LC-MS method with electrospray ionization for quantitation of digoxin in human plasma and urine: Application to a pharmacokinetic study. J Chromatogr B Analyt Technol Biomed Life Sci, 15(875), 2.

Smith, Mark (2016). "So you think you chose to read this article?". BBC News. Archived from the original on 25 July 2016.

Sugiyama, T., Matsuyama, R., Usui, S., Katagiri, Y., & Hirano, K. (2000). Selection of mobile phase in high-performance liquid chromatographic determination for medicines. Biological and Pharmaceutical Bulletin, 23(3), 274-278.

Švancara, I., Galík, M., & Vytřas, K. (2007). Stripping voltammetric determination of platinum metals at a carbon paste electrode modified with cationic surfactants. Talanta, 72(2), 512-518.

švancara, I., Kalcher, K., Diewald, W., & Vytřas, K. (1996). Voltammetric determination of silver at ultratrace levels using a carbon paste electrode with improved surface characteristics. Electroanalysis, 8(4), 336-342.

Teha, A. S., & Koh, P. Y. (2009). Synthesis, properties, and applications of magnetic iron oxide nanoparticles. Progress in crystal growth and characterization of materials, 55(1-2), 22-45.

Todorovi Ć, Z. B., Lazi Ć, M. L., Veljkovi Ć, V. B., & Milenovi Ć, D. M. (2009). Validation of an HPLC-UV method for the determination of digoxin residues on the surface of manufacturing equipment. Journal of the Serbian Chemical Society, 74(10).

Varma, M. V., Kapoor, N., Sarkar, M., & Panchagnula, R. (2004). Simultaneous determination of digoxin and permeability markers in rat in situ intestinal perfusion samples by RP-HPLC. Journal of Chromatography B, 813(1-2), 347-352.

Vinay, M., & Nayaka, Y. A., Journal of Science: Advanced Materials and Devices, 4(3), (2019) 442-450.

Vytřas, K., Švancara, I., & Metelka, R. (2009). Carbon paste electrodes in electroanalytical chemistry. Journal of the Serbian Chemical Society, 74(10), 1021-1033.

Wan, J., Chen, X., Wang, Z., Yang, X., & Qian, Y. (2005). A soft-template-assisted hydrothermal approach to single-crystal Fe3O4 nanorods. Journal of Crystal Growth, 276(3-4), 571-576.

Willard, M. A., Kurihara, L. K., Carpenter, E. E., Calvin, S., & Harris, V. G. (2004). Chemically prepared magnetic nanoparticles. International materials reviews 49(3-4), 125-170.

Wu, W., He, Q., & Jiang, C. (2008). Magnetic iron oxide nanoparticles: synthesis and surface functionalization strategies. Nanoscale research letters, 3(11), 397.

Zhao, Z., Zhou, Z., Bao, J., Wang, Z., Hu, J., Chi, X., ... & Gao, J. (2013). Octapod iron oxide nanoparticles as high-performance T 2 contrast agents for magnetic resonance imaging. Nature communications, 4, 2266.

Xie, W., Guo, Z., Gao, F., Gao, Q., Wang, D., Liaw, B. S., ... & Zhao, L. (2018). Shape-, size-and structure-controlled synthesis and biocompatibility of iron oxide nanoparticles for magnetic theranostics. Theranostics, 8(12), 3284.

Gmelin, Leopold (1822). [On a particular potassium iron cyanate, and on a new series of iron salts of cyanic acid]. Journal für Chemie und Physik (in German). 34: 325–346.

Carson, F. L. (1997). Histotechnology: A Self-Instructional Text (2nd ed.). Chicago: American Society of Clinical Pathologists. pp. 209–211.

Drexler, K. Eric (1986). Engines of Creation: The Coming Era of Nanotechnology. Doubleday. ISBN 978-0-385-19973-5.

Park M., Im J., Shin M., Min Y., Park J., Cho H., Park S., Shim M.B., Jeon S., Chung D.Y., et al. Highly stretchable electric circuits from a composite material of silver nanoparticles and elastomeric fibres. Nat. Nanotechnol. 2012;7:803–809. doi: 10.1038/nnano.2012.206.

Kissinger, P. T., Heineman, W. R., "Cyclic Voltammetry," Journal of Chemical Education, 60, 702 (1983).

A.J. Bard, L.R. Faulkner Electrochemical Methods, Fundamental and Applications

Wiley, New York (2001)

Breiman, L. (June 1997). "Arcing the Edge" (PDF). Technical Report 486. Statistics Department, University of California, Berkeley.

Friedman, J. H. (February 1999). "Greedy Function Approximation: A Gradient

Boosting Machine" (PDF).

Panahi, Y.; Motaharian, A.; Hosseini, M.R.M.; Mehrpour, O. High sensitive and selective nano-molecularly imprinted polymer based electrochemical sensor for midazolam drug detection

in pharmaceutical formulation and human urine samples. Sens. Actuators B Chem. 2018, 273, 1579–1586

John O'M. Bockris, Fuel Cells: Their Electrochemistry; Surface Electrochemistry, 1969.

Aleksandar R. Despić and V. D. Jovic, Modern Aspects of Electrochemistry, 1995.

Kissinger, P. T. & Heinemann, W. R. (1996). Laboratory techniques in electroanalytical chemistry. Marcel Dekker, Inc., New York, 2nd edition.pp 254 - 255.

Wang, J. (2006). Analytical Electrochemistry (2nd Ed.). New York: Wiley-VCH.

jelechem_2019 Journal of Electroanalytical Chemistry, 10.1016/j,113405, (113405).

Wiley New York (2004) 375–461.  C. Kötting, W. Sander, J. Am. Chem. Soc. 121, 8891 .

**APPENDICES**

# APPENDIX 1

## SIMILARITY REPORT

| AUTHOR ▲ | TITLE | SIMILARITY | |
|---|---|---|---|
| Najiya Maroof | abstract | 0% | |
| Najiya Maroof | All thesis chapters | 11% | |
| Najiya Maroof | chapter1 | 6% | |
| Najiya Maroof | chapter2 | 13% | |
| Najiya Maroof | chapter3 | 14% | |
| Najiya Maroof | chapter4 | 13% | |
| Najiya Maroof | chapter5 | 0% | |
| Najiya Maroof | chapter6 | 0% | |

Yrd. Doç. Dr. Süleyman Aşır

NAJIYA MAROOF SALEEM

# APPENDIX 2

**ETHICAL APPROVAL DOCUMENT**

NEAR EAST UNIVERSITY

**ETHICAL APPROVAL DOCUMENT**

Date: / /2021

**To the Instıtute of Graduate Studies**

For the thesis project entitled as "Effect of $Fe_3O_4$ nanoparticles on the prediction of Ferricyanide concentration by Carbon paste electrode using artificial neutral networks" the researchers declare that they did not collect any data from human/animal or any other subjects. Therefore, this project does not need to go through the ethics committee evaluation

Title: **Asst**. **Prof. Dr.**

Name Surname: **Süleyman Aşır**

Signature:

Role in the Research Project: **Supervisor**